ADVANCED ASYNCHRONOUS RANDOM ACCESS PROTOCOLS

A THESIS SUBMITTED TO
THE GRADUATE SCHOOL OF ENGINEERING AND SCIENCE
OF BILKENT UNIVERSITY
IN PARTIAL FULFILLMENT OF THE REQUIREMENTS FOR
THE DEGREE OF
MASTER OF SCIENCE
IN
ELECTRICAL AND ELECTRONICS ENGINEERING

By
Talha Akyıldız
August 2020

Advanced Asynchronous Random Access Protocols
By Talha Akyıldız
August 2020

We certify that we have read this thesis and that in our opinion it is fully adequate, in scope and in quality, as a thesis for the degree of Master of Science.

Tolga Mete Duman (Advisor)

Nail Akar

Ayşe Melda Yüksel Turgut

Approved for the Graduate School of Engineering and Science:

Ezhan Karaşan
Director of the Graduate School

ABSTRACT

ADVANCED ASYNCHRONOUS RANDOM ACCESS PROTOCOLS

Talha Akyıldız
M.S. in Electrical and Electronics Engineering
Advisor: Tolga Mete Duman
August 2020

Fifth generation wireless systems and beyond require linking an enormous number of simple machine type devices leading to a new wave of interest in massive machine type communications (mMTC). Different from the human-centric communication systems, mMTCs are composed of a large number of devices where each user node generates small data blocks sporadically in an unpredictable manner. In such scenarios, traditional multiple access schemes, e.g., time division multiple access or frequency division multiple access, are not suitable because resource allocation and scheduling based approaches cannot be conveniently adopted due to the required complexity and latency, motivating the use of uncoordinated random access (RA) protocols and making asynchronous ALOHA-like solutions ideal candidates for such applications.

In this thesis, we consider the design and analysis of advanced asynchronous RA protocols for different settings. We first study contention resolution ALOHA (CRA) and irregular repetition ALOHA (IRA) protocols with regular and irregular repetition rates on the collision channel where collisions are resolved through successive interference cancellation. We also propose concatenation of packet replicas with some clean parts with IRA, named irregular repetition ALOHA with replica concatenation (IRARC). Secondly, we introduce energy harvesting (EH) into the framework with the motivation of self-sustainability, and study RA protocols with EH nodes. Finally, we propose a generalization of IRA with packet length diversity to improve the system performance further. We present asymptotic analyses of all the proposed RA protocols, and determine the optimal repetition distributions to maximize the system throughput. We also provide a comprehensive set of numerical results for both asymptotic and practical scenarios to further demonstrate the effectiveness of the proposed approaches.

Keywords: Random access, contention resolution ALOHA, irregular repetition ALOHA, asymptotic analysis, successive interference cancellation, energy harvesting.

ÖZET

GELİŞMİŞ ASENKRON RASTGELE ERİŞİM PROTOKOLLERİ

Talha Akyıldız
Elektrik ve Elektronik Mühendisliği, Yüksek Lisans
Tez Danışmanı: Tolga Mete Duman
Ağustos 2020

Beşinci nesil kablosuz sistemler ve ötesi çok sayıda basit makine tipi cihazın bağlanmasını gerektirmektedir ve bu durum masif makine tipi iletişimlerine (mMTCs) karşı yeni bir ilgi dalgasına yol açmaktadır. İnsan merkezli iletişim sistemlerinden farklı olarak mMTC'ler, her kullanıcı düğümünün öngörülemeyen bir şekilde düzensiz olarak küçük veri blokları ürettiği çok sayıda cihazdan oluşur. Bu tür senaryolarda, geleneksel çoklu erişim şemaları, örneğin zaman bölmeli çoklu erişim veya frekans bölmeli çoklu erişim uygun değildir, çünkü gerekli karmaşıklık ve gecikme nedeniyle kaynak tahsisi ve programlamaya dayalı yaklaşımlar uygun şekilde uygulanamaz. Bu durum koordineli olmayan rastgele erişim (RA) protokollerinin kullanımını motive etmekte ve asenkron ALOHA benzeri çözümleri bu tür uygulamalar için ideal adaylar haline getirmektedir.

Bu tezde, gelişmiş asenkron RA protokollerinin tasarımını ve analizini farklı ayarlar için ele alıyoruz. İlk olarak, çarpışmaların ardışık girişim iptali ile çözüldüğü çarpışma kanalında düzenli ve düzensiz tekrar oranlarına sahip çekişme çözünürlüğü ALOHA (CRA) ve düzensiz tekrarlı ALOHA (IRA) protokollerini inceliyoruz. Ayrıca, IRA ile paket kopyalarının temiz parçalarının bir araya getirildiği replika birleştirmesi ile düzensiz tekrarlı ALOHA (IRARC) adlı şemayı öneriyoruz. İkinci olarak, kendi kendine sürdürülebilirlik motivasyonu ile enerji hasadını (EH) sisteme dahil ediyoruz ve RA protokollerini EH düğümleriyle çalışıyoruz. Son olarak, sistem performansını daha da iyileştirmek için IRA'nın paket uzunluğu çeşitliliği ile genellemesini öneriyoruz. Önerilen tüm RA protokollerinin asimptotik analizlerini sunuyoruz ve sistem verimini maksimize etmek için optimum tekrar dağılımlarını belirliyoruz. Ayrıca, önerilen yaklaşımların etkinliğini daha da göstermek için hem asimptotik hem de pratik senaryolar için kapsamlı bir sayısal sonuç seti sunuyoruz.

Anahtar sözcükler: Rastgele erişim, çekişme çözünürlüğü ALOHA, düzensiz tekrarlı ALOHA, asimptotik analiz, ardışık girişim iptali, enerji hasatlama.

Acknowledgement

First and foremost, I would like to express my deepest gratitude and appreciation to my advisor Prof. Tolga M. Duman for his endless support, encouragement, and patience. He has always been an excellent advisor and a role model to me. I feel very fortunate to work with him for three years and it would not be possible to conduct this research without him.

I would like to thank Prof. Nail Akar and Assoc. Prof. Ayşe Melda Yüksel Turgut for accepting to serve as my examining committee members and for their valuable comments.

I also acknowledge the financial support of The Scientific and Technological Research Council of Turkey (TÜBİTAK) under the 2210-A program with sincere gratitude.

I have been extremely fortunate to be surrounded constantly by İbrahim Kurban Özaslan and Cüneyd Öztürk. I would like to thank them for our conversations and amusing breaks.

I would also like to thank the members of the Bilkent Communication Theory and Application Research (CTAR) Lab, Büşra Tegin, Mert Özateş, Sadra Charandabi, Mahdi Shakiba Herfeh, Sina Rezaei Aghdam, and Mehdi Dabirnia.

Last but not least, I would like to express my gratitude to my beloved family for their precious support.

Contents

List of Figures

List of Tables

List of Abbreviations

AWGN additive white Gaussian noise.

CRA contention resolution ALOHA.

CRARC contention resolution ALOHA with replica concatenation.

CRDSA contention resolution diversity slotted ALOHA.

CSA coded slotted ALOHA.

CSMA carrier sense multiple access.

DAMA demand assignment multiple access.

DFA dynamic framed ALOHA.

DSA diversity slotted ALOHA.

EH energy harvesting.

EH-IRSA energy harvesting irregular repetition slotted ALOHA.

FA framed ALOHA.

FEC forward error correction.

IRA irregular repetition ALOHA.

IRA-PLD irregular repetition ALOHA with packet length diversity.

IRARC irregular repetition ALOHA with replica concatenation.

IRSA irregular repetition slotted ALOHA.

LDPC low density parity check.

M2M machine to machine.

MAC medium access control.

mMTC massive machine type communications.

MTD machine type device.

PLR packet loss rate.

PMF probability mass function.

RA random access.

SIC successive interference cancellation.

SINR signal-to-interference noise ratio.

TDMA time division multiple access.

Chapter 1

Introduction

1.1 Overview

With the foreseen proliferation of machine type devices (MTDs), machine to machine (M2M) communications have recently attracted great interest for 5G wireless systems and beyond. In massive M2M communications, the number of users is extremely high; users are only sporadically active in an unpredictable manner and they are equipped with low complexity and low energy consuming simple MTDs [1, 2]. These requirements pose compelling challenges that need to be overcome with a suitable access mechanism. Existing multiple access protocols, e.g., demand assignment multiple access (DAMA) or time division multiple access (TDMA), cannot meet the requirements of massive M2M communications due to the signaling and control overhead which increases with the network size. In addition, carrier sense multiple access (CSMA) demands steady channel sensing and some of its variants require a feedback mechanism to access the channel, hence it is not favorable for a network of a very large number of low complexity MTDs.

Random access (RA) is well-suited for M2M communications as it can accommodate a massive number of users with sporadic activity. That is, as the

number of active users at a certain time is limited, RA allows users to access the medium without any prior request in an uncoordinated manner. Basic RA schemes, ALOHA and slotted ALOHA, enable users to share the channel without any coordination and permission, however, they suffer from inevitable collisions that result in an inferior system performance. On the other hand, advanced random access (RA) approaches promise convenient and elegant solutions for M2M communications providing promising increased system performance, especially with the utilization of successive interference cancellation (SIC) techniques [3]. In this setting, while synchronous RA schemes provide better performance by taking the advantage of slot level synchronization, due to the challenges in achieving such a synchronization, advanced asynchronous schemes are also appealing, and they should be investigated in detail.

In massive M2M communications, another important aspect is the long-term operation capability of the system. As replacing batteries of a massive number of MTDs is not viable, there is a need for energy-autonomous systems. To this end, energy harvesting (EH) appears as a promising solution, providing self-sustainability and perpetual operation with energy harvested from the environment [4]. Moreover, thanks to the sporadic activity of the MTDs, a continuous use of a high level of energy is not required, which allows MTDs to operate with a low-energy consumption over the long-term making EH a favorable option. Since stochastic nature of the available energy in EH systems deteriorates the system performance in standard RA schemes, the design and analysis of such schemes should be carried out by paying attention to the energy limitations.

With this motivation, in this thesis, we explore the design and analysis of advanced asynchronous RA protocols. We first study CRA and IRA protocols by conducting asymptotic performance analysis. We also present an extension by employing replica concatenation, resulting in IRARC. We then propose a practical adaptation of IRA and IRARC with EH nodes. Finally, we consider IRA with packet length diversity to improve the system performance further.

1.2 Contributions of the Thesis

The main aim of this thesis is to provide a detailed investigation of asynchronous RA schemes under various settings and different considerations. Specifically, we are interested in optimizing the asymptotic performance of asynchronous RA schemes via analytical tools. Specific contributions of the thesis are summarized below.

We develop an asymptotic analysis of CRA over the collision channel assuming that collisions are resolved through successive interference cancellation (SIC). Initially, we consider regular repetition rates, and then we generalize our approach to irregular repetition distributions. We refer to the latter scheme as IRA [1]. Via the proposed analysis, we observe that introducing irregular repetition rates offers higher asymptotic throughputs. We also consider an advancement of CRA/IRA by concatenation of clean parts of different replicas in partial collisions to improve the system throughput. We extend our analysis, which is amenable for further extensions, to this scheme as well. In addition, we verify the accuracy of the asymptotic analytical results through finite length simulations.

We then consider an adaptation of IRA and IRARC to the case with energy harvesting nodes equipped with finite-sized batteries. We specify the system design parameters and provide an asymptotic analysis for this scenario by taking the stochasticity of energy arrivals into account. We derive the optimal packet repetition distributions based on the available energy in the battery to maximize the asymptotic throughput. The asymptotic results are corroborated with finite length simulations. Furthermore, we also compare the performance of the proposed approach with two different alternatives to demonstrate its advantages.

Finally, we study an asynchronous RA scheme where the users are allowed to generate different length packets with different repetition rates over a collision channel with the motivation that users are not restricted to transmit their packets with equal lengths. We explore this idea and show that the approach may be used

[1] IRA is s a generalization of CRA with varying repetition rates. CRA can be considered as a special case of IRA with fixed repetition rates.

as a source of further diversity potentially improving the system performance. We develop an asymptotic analysis of the newly proposed scheme by extending the analysis technique of IRA. With the help of the developed approach, we perform optimization over both repetition rates and packet durations, and determine the packet length and repetition distributions that maximize the normalized throughputs. The results demonstrate that the proposed scheme achieves significantly higher asymptotic throughputs compared to IRA, and hence, the additional diversity offered by the use of different packet lengths is highly beneficial. We also perform simulations to confirm our findings for practical scenarios with finite frame lengths.

Our results in this thesis are reported in two published conference papers and one submitted journal paper:

- T. Akyıldız, U. Demirhan and T. M. Duman, "Asymptotic analysis of contention resolution ALOHA with replica concatenation," in *Proc. IEEE Int. Conf. Commun. (ICC),* Shanghai, China, May 2019. [5]
- T. Akyıldız and T. M. Duman, "Irregular repetition ALOHA with packet length diversity," in *Proc. IEEE Glob. Telecommun. Conf. (GLOBECOM),* Waikoloa, HI, USA, Dec. 2019. [6]
- T. Akyıldız, U. Demirhan and T. M. Duman, "Energy Harvesting Irregular Repetition ALOHA with Replica Concatenation," *IEEE Trans. Wirel. Commun.,* (under revision).

1.3 Thesis Outline

The rest of this thesis is organized as follows. In Chapter 2, we provide the fundamentals of basic and advanced RA schemes along with some required mathematical tools as well as comparative simulation results. In Chapter 3, we describe the main system model of CRA and IRA and develop an asymptotic analysis of CRA and IRA. The analysis is then extended for the replica concatenation scenario

CRARC/IRARC, and optimized repetition distributions and numerical results with finite length simulations are given. In Chapter 4, the design and analysis of IRA and IRARC with energy harvesting nodes are studied. We derive an optimal transmission policy in order to maximize the overall system throughput. We also perform simulations for practical scenarios. In Chapter 5, we propose an analysis for irregular repetition ALOHA with packet length diversity (IRA-PLD). We optimize the probability distributions of packet lengths and repetition rates, and provide the corresponding asymptotic system performance in comparison with that of IRA. Numerical results of our findings through finite length simulations are also given. Finally, we present our conclusions and directions for future research in Chapter 6.

Chapter 2

Preliminaries and Literature Review

This chapter is intended as a short background for the subsequent chapters explaining the fundamental concepts in our study of RA protocols. We first present an overview of basic RA protocols along with their performance evaluations. We then review the related (advanced) synchronous and asynchronous RA schemes. We also review the existing works on RA with energy harvesting nodes.

The chapter is organized as follows. In Section 2.1, ALOHA, slotted ALOHA and diversity slotted ALOHA (DSA) protocols are explained. Section 2.2 presents other synchronous RA protocols with a focus on CRDSA and IRSA. Section 2.3 reviews the related asynchronous advanced RA protocols, namely, CRA, ECRA and ACRDA. Section 2.4 reviews the ALOHA based RA protocols with energy harvesting. Section 2.5 concludes the chapter with a table including the related advanced RA protocols with their main features.

2.1 Basic RA Schemes

2.1.1 ALOHA

ALOHA [7] is a pioneering computer networking system developed by Abrahamson to connect multiple computers (nodes) to a common receiver. In ALOHA, the multiaccess medium is accessed among various nodes in an uncoordinated manner. Each node accesses the medium immediately whenever it has a packet to transmit without any permission or prior request (grant-free). During this access or transmission, medium can be in two states: 1) it might be busy: some other nodes are transmitting; 2) it might be free: none of the remaining nodes are transmitting. In the former case, a collision occurs and the transmitted packet cannot be received correctly. The receiver sends an immediate feedback to user and the user retransmits the collided packet after a random delay. In the latter case, a packet encounters no interference and it is received perfectly. After successful transmission, the user waits for a new packet arrival for its next transmission.

Let us assume that a specific packet is transmitted at time instant t, and that all the packets have the same length τ. If there is no other transmission in the interval $[t-\tau, t+\tau]$, the transmitted packet will be received successfully. However, if there is at least one another transmission in this interval, the packet will be lost. This interval is also known as a *vulnerable period* of this specific replica. Consider the illustration given in Fig. 2.1 which shows that the first user's second packet is transmitted at time instant t, and it needs to be retransmitted after some random amount of time due to the transmission of the second user's first packet inside its vulnerable period.

For a simple mathematical analysis of ALOHA, we denote the number of users by N and we use an infinite node model ($N \to \infty$) [1]. This assumption allows us to model the new packet arrivals by a Poisson process with rate λ. Assuming that the retransmissions of packets are randomized sufficiently, the number of total packet arrivals, including the new arrivals and retransmissions, is a Poisson random

[1] A more precise model of ALOHA is also possible by a discrete-time Markov chain [8].

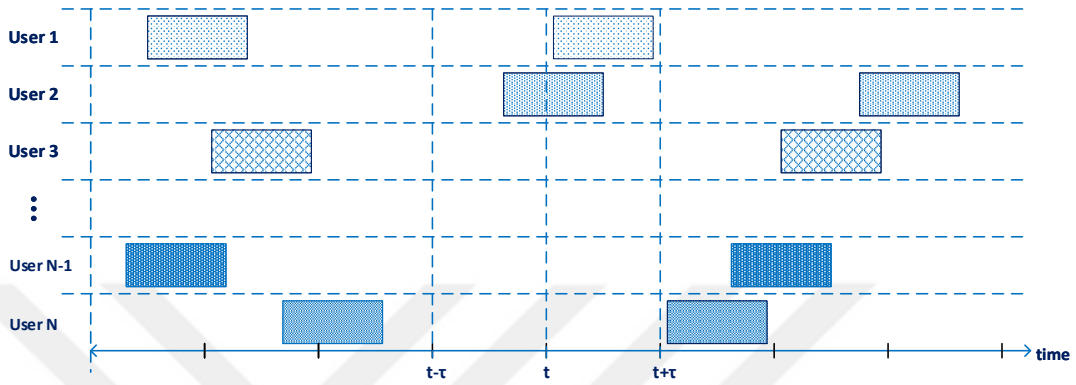

Figure 2.1: A visualization of ALOHA protocol for N users over time.

variable with density G, i.e., $G > \lambda$. G is the channel load and corresponds to the expected total number of arrivals per packet duration τ [packet/packet duration].

We note that the length of the vulnerable period is equal to the two packet lengths, 2τ, and a successful transmission is only possible if there are no packet arrivals inside this interval. Hence, we can write the probability of a successful transmission denoted by p_s as

$$\begin{aligned} p_s &= \Pr\{\text{No packet arrivals inside the interval of length } 2\tau\} \\ &= e^{-2G}. \end{aligned}$$

We next compute the throughput, T, defined as the expected number of users successfully received per packet duration which is a simple multiplication of G and p_s,

$$T = Ge^{-2G} \text{ [packet/packet duration]}. \tag{2.1}$$

The maximum throughput is obtained when $G = 0.5$ (which can be found by taking the derivative of T with respect to G), and the normalized peak throughput is $1/2e \approx 0.18$. We observe that the channel efficiency is quite low for pure ALOHA due to the uncoordinated nature of the protocol and lack of synchronization.

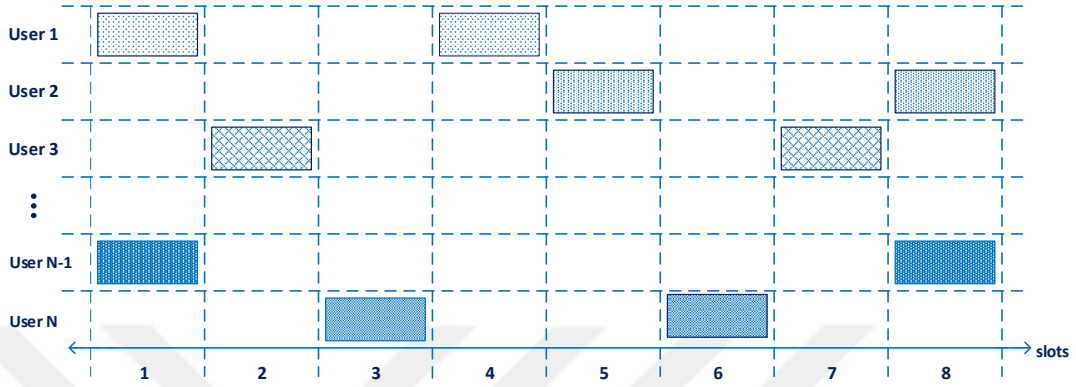

Figure 2.2: A visualization of slotted ALOHA protocol for N users over time.

2.1.2 Slotted ALOHA

Slotted ALOHA is developed by Roberts by introducing slot synchronization to ALOHA [9]. In slotted ALOHA, time is divided into time slots with an equal duration of packet length τ. Hence, transmissions can only occur in these specific time slots dissimilar to pure ALOHA. Due to the synchronization, a packet is collided only if there is another transmission at the same slot. Again, if we consider a specific packet is sent at time instant t, the vulnerable of this packet is $[t, t+\tau]$. An illustration of packet transmissions from N users for slotted ALOHA is given in Fig. 2.2.

With slotted ALOHA, the length of the vulnerable period of a packet is decreased from 2τ to τ thanks to the slot synchronization. However, it should be noted that this synchronization leads to higher delays since users have to wait for the beginning of the next slot for transmission. We define G as the expected number of total packet arrivals per slot [packet/slot], and write the probability of a successful transmission for slotted ALOHA as

$$\begin{aligned} p_s &= \Pr\{\text{No packet arrivals inside the interval of length } \tau\} \\ &= e^{-G}. \end{aligned}$$

The throughput definition is similar to ALOHA and defined as the expected

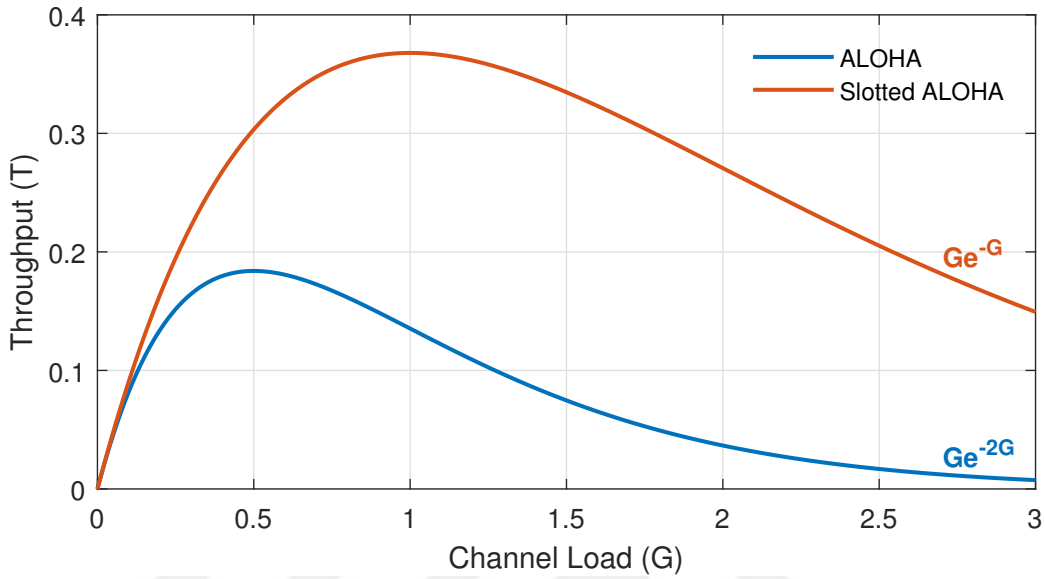

Figure 2.3: The throughput performance comparison of ALOHA and slotted ALOHA for different values of G.

number of packets received correctly per time slot,

$$T = Ge^{-G} \text{ [packet/slot]}, \tag{2.2}$$

which is maximized for $G = 1$ with a peak value of $= 1/e \approx 0.37$. The maximum throughput is doubled compared to that of ALOHA, which is due to the fact that the use of slots decreases the probability of collisions, and hence, it increases the channel efficiency.

We provide the throughput comparison of ALOHA and slotted ALOHA as a function of the channel load in Fig. 2.3.

As an extension of pure ALOHA and slotted ALOHA, diversity slotted ALOHA (DSA) introduces packet repetitions to slotted ALOHA, i.e., each user transmits the same packet twice, instead of once [10]. In this scheme, a packet can be recovered if one of its repetitions is transmitted successfully. The idea is to increase the improve the throughput and lower transmission delay. This scheme is beneficial for low load values (a small number of users), however, it is outperformed by slotted ALOHA at high load values.

2.2 Advanced Synchronous RA Schemes

2.2.1 CRDSA and IRSA

Long after the introduction of ALOHA and slotted ALOHA, contention resolution diversity slotted ALOHA (CRDSA) has been introduced. CRDSA adopts the idea of transmitting a packet with an additional copy (as in DSA) and employs SIC on the collision channel [3]. With the use of diversity and SIC together, the collisions are not simply *lost* anymore. Even when a packet experiences a collision, if its other copy is collision free, then the interference of the collided copy can be removed from the frame which allows the receiver to possibly decode the other collided packets as well. The use of SIC leads to a notable performance improvement, enhancing the maximum normalized throughput to $T \approx 0.55$. As an advancement of the original version of CRDSA, with CRDSA++ [11], transmitting more than one copy is shown to improve the system performance further, with a maximum normalized throughput of ≈ 0.68 and ≈ 0.772 by transmitting 2 and 3 additional copies, respectively.

More recently, IRSA has been developed as an extension of CRDSA by considering irregular repetition rates, instead of only fixed repetitions in [12]. A major contribution of [12] is the asymptotic throughput analysis for given repetition distributions through a graph-based approach, exploiting the similarity with the technique of density evolution employed in the analysis and design of low density parity check (LDPC) codes. By utilizing the proposed analysis, repetition rates can be optimized via a differential evolution algorithm [13] leading to higher maximum asymptotic normalized throughput values, up to nearly 1.

In this subsection, we present the system model of CRDSA and IRSA, and then review the converge analysis of IRSA (which also covers the case of CRDSA). We also provide numerical examples via finite frame length simulations to evaluate and compare the performance of these two RA schemes.

2.2.1.1 System Model

The time is divided into MAC frames with a duration of T_f. Each MAC frame consists of M time slots with an equal duration of τ, i.e., $M = T_f/\tau$. Packet transmissions can only occur within the slots. Therefore, the packet length is equal to the duration of a slot. Each user attempts a single packet transmission over a MAC frame with regular or irregular repetitions. The transmission time of replicas are uniformly distributed over the duration of the frame independently. A transmission may be a new packet arrival or retransmission of a collided packet from the previous MAC frames. The number of users (packets) is denoted by N. The normalized load is defined as the expected number of packets per slot and denoted by G, i.e., $G = N/M$. The normalized throughput T is the probability of a packet not being collided for a given slot.

In CRDSA and IRSA, a collision channel model is adopted. In this model, the receiver is able to detect the slots with no packet, a single packet and multiple packet transmissions. Multiple transmissions result in collisions and none of the packets can be decoded unless the interference due to the other packets is removed. Single packet transmission is always decoded successfully since there are no interfering packets in the slot. Each packet replica contains a header where the position of other replicas is located. This location information allows the receiver to utilize SIC. Hence, after successful decoding of a packet, the receiver can remove the interference of all of its replicas from the frame using the location information and utilize SIC. This interference cancellation process continues iteratively, and it enables the receiver to resolve some or possibly all the packets experiencing collisions.

An example from a MAC frame of IRSA is given in Fig. 2.4 with N users and M slots. User 1 transmits its packet with 3 replicas, while users 2 and 3 only transmit 2 replicas [2]. In this example, we briefly explain the benefit of SIC operation as follows. The second slot contains only a single packet replica, hence user 1's first replica can be successfully decoded, and the interference of

[2]We note that all users transmit 2 replicas in CRDSA. Hence, it can be considered as a special case of IRSA with fixed repetition rates.

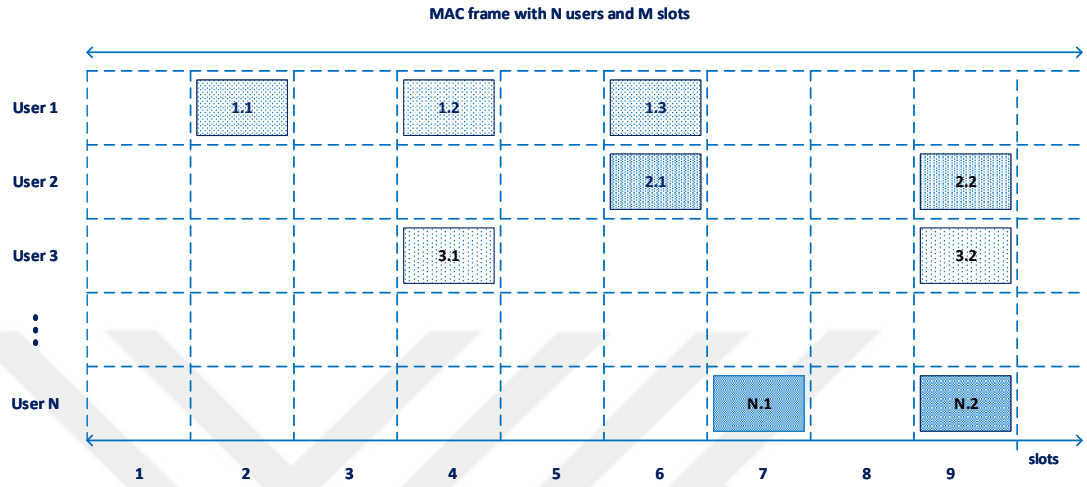

Figure 2.4: A visualization of MAC frame for IRSA with N users and M slots.

the replicas 1.2 and 1.3 in the 4-th and 6-th slots can be removed. Then, user 2 and user 3's first replicas become interference free and they can be resolved successfully. Hence, even though users 2 and 3 do not have any replicas without collisions at the beginning, their packets become interference free and can be decoded via SIC iterations.

The SIC mechanism is now described through a bipartite graph representation of a MAC frame with N users and M slots. A bipartite graph is denoted by $\mathcal{G} = (B, S, E)$, where B is the set of N burst nodes (BNs), S is the set of M sum nodes (SNs), and E is the set of edges connecting a BN to SN. In this graph representation, BNs and SNs correspond to users and slots, respectively. Specifically, a user with l replicas is represented by a BN with l connections (node degree). Similarly, a slot with l replica arrivals is represented by an SN with l connections.

An example of a MAC frame and the corresponding bipartite graph representation of IRSA with 4 users and 4 slots is given in Fig. 2.5. A BN is connected to an SN if the user has a replica in the corresponding slot. For example, user 1 transmits its replicas in the first and third slots, and hence, BN 1 (B_1) is connected to SNs 1 and 3 (S_1 and S_3). We now describe the SIC process in an iterative manner as depicted in Fig. 2.6. At the first iteration, only the second user has a clean

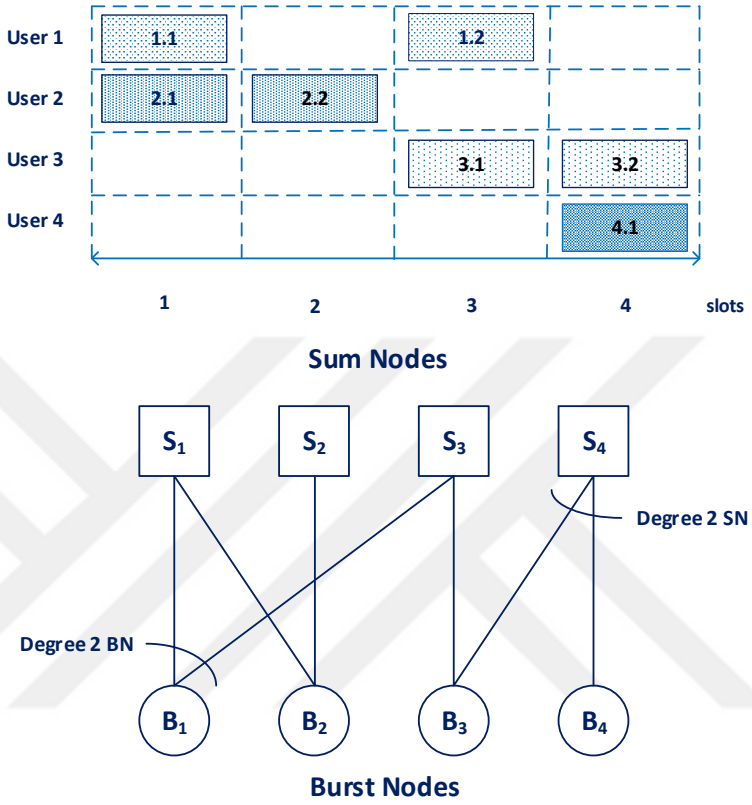

Figure 2.5: A MAC frame and its corresponding bipartite graph representation with 4 users and 4 slots.

replica in the second slot which can be decoded successfully and its interference in the first slot is subtracted. Then, user 1's first replica becomes interference free and it can be resolved. The receiver cancels its interference contribution in slot 3. At the third iteration, slot 3 only contains the replica belonging to the user 3, and hence the replica can be decoded. Finally, after removing the interference of user 3, the packet of user 4 can be recovered successfully.

In the bipartite graph representation, the probability that a burst node has l connections, i.e., a user transmitting l replicas, is denoted by Λ_l. Similarly, let Ψ_l denote the probability that a sum node has l connections, i.e., a slot having l replica arrivals, as well. The BN and SN degree distributions can be represented

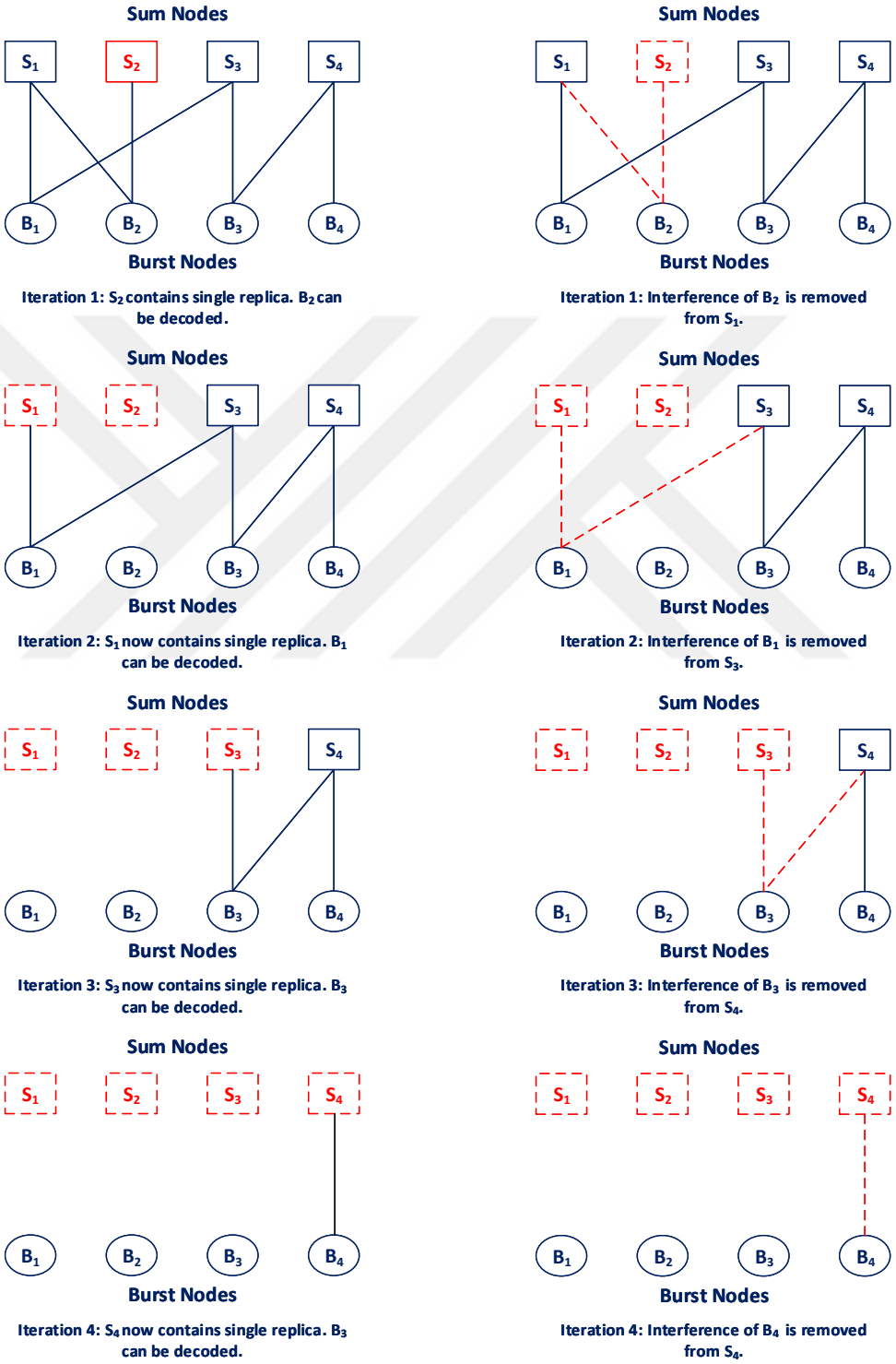

Figure 2.6: SIC process of IRSA through bipartite graph representation with 4 users and 4 slots.

in a polynomial form as

$$\Lambda(x) \triangleq \sum_l \Lambda_l x^l, \qquad \Psi(x) \triangleq \sum_l \Psi_l x^l. \tag{2.3}$$

The average number of connections for BN and SN are given by $\sum_l l\Lambda_l = \Lambda'(1)$ and $\sum_l l\Psi_l = \Psi'(1)$, respectively. $\Lambda'(1)$ is the average packet repetition rate and $\Psi'(1)$ is the average number of replica arrivals in a slot in a MAC frame. Recalling the definition of G, we can write $G = N/M = \Psi'(1)/\Lambda'(1)$.

It is also possible to define the degree distributions from an edge perspective. Let λ_l denote the probability that an edge is connected to a BN with l connections. Likewise, ρ_l denotes the probability that an edge is connected to an SN with l connections. The edge perspective probabilities can be written in terms of Λ_l and Ψ_l as

$$\lambda_l = \frac{l\Lambda_l}{\sum_l l\Lambda_l}, \qquad \rho_l = \frac{l\Psi_l}{\sum_l l\Psi_l}. \tag{2.4}$$

The corresponding edge degree distributions can be written as follows

$$\lambda(x) \triangleq \sum_l \lambda_l x^{l-1}, \qquad \rho(x) \triangleq \sum_l \rho_l x^{l-1}, \tag{2.5}$$

and they can be related to the node degree distributions by $\lambda(x) = \Lambda'(x)/\Lambda'(1)$ and $\rho(x) = \Psi'(x)/\Psi'(1)$.

2.2.1.2 Convergence Analysis

In this subsection, we review a convergence analysis technique developed in the literature, and it allows us to derive the average erasure probabilities of edges through the SIC iterations, and hence makes it possible to assess the asymptotic throughput of the random access schemes. The analysis can be performed using the node and edge degree distributions, that is, through the analysis, the normalized throughput and packet loss rate for a given $\Lambda(x)$ can be computed. Then, the repetition rates can be optimized to maximize the normalized throughput via a technique called differential evolution [13].

Differential evolution is a stochastic and population based evolutionary optimization algorithm. The algorithm is developed to optimize a given real-valued objective function with multiple continuous variables. The evolutionary algorithm contains 4 steps which is described as follows: *1) Initialization:* Select an initial vector with the uniformly distributed variables over the search space. *2) Mutation:* Select at least three different new candidates randomly. Then, obtain a donor vector with the weighted linear combination of the selected candidates. *3) Recombination:* In this step, the donor vector is accepted as a trial vector with some cross-over probability. Otherwise, the initial vector becomes the trial vector. *4) Selection:* Finally, if the trial vector performs better, the initial vector is replaced by the trial vector. The steps 2, 3 and 4 are performed until some stopping criteria is reached. At the end, well-performing solutions can be obtained, but of course, differential evolution does not guarantee a globally optimal solution.

Let q denote the probability of an edge connected to a BN with degree l being unknown. Also, let p be the probability of an edge connected to an SN with degree l being unknown. For a BN with degree l, an edge can be revealed if at least one of the remaining edges is known from the previous iteration step. In other words, a packet with l replicas can be decoded by the receiver if at least one of the replicas does not experience collision. Hence, we can write q in terms of p as $q = p^{l-1}$. Similarly, for an SN with degree l an edge can be revealed if all of the remaining edges is known from the previous iteration step. Particularly, a replica inside a slot with l arrivals can be resolved only if the remaining $l-1$ arrivals are resolved. Hence, we can write p in terms of q as $p = 1-(1-q)^{l-1}$. The average probabilities can be obtained using the edge degree distributions during the iteration i, i.e.,

$$q_i = \sum_l \lambda_l p_{i-1}^{l-1} = \lambda(p_{i-1}), \tag{2.6}$$

and

$$p_i = \sum_l \rho_l \big(1-(1-q_i)^{l-1}\big) = 1-\rho(1-q_i), \tag{2.7}$$

where i denotes the iteration number. The convergence analysis can be performed iteratively using (2.6) and (2.7), i.e., $p_i = 1-\rho(1-\lambda(p_{i-1}))$ with an initial values,

$q_0 = p_0 = 1$. It should be noted that the relationship between q_i and p_i is only accurate under the condition that the statistics of edges are independent from each other. Hence, the convergence analysis requires asymptotic settings, $N, M \to \infty$ for a constant G.

To complete the analysis, SN degree distributions $\Psi(x)$ and $\rho(x)$ need to be derived. As a first step, we calculate the probability Ψ_l. The average replica arrival per slot is given by $\Psi'(1)$ and the probability that a user transmits a replica in a given slot is $\Psi'(1)/N$ since the transmission times are uniformly distributed. The probability of a slot having l replica arrivals follows a binomial distribution with probability $\Psi'(1)/N$, i.e.,

$$\Psi_l = \binom{N}{l} \left(\frac{\Psi'(1)}{N}\right)^l \left(1 - \frac{\Psi'(1)}{N}\right)^{N-l}.$$

The corresponding degree distribution $\Psi(x)$ using (2.3) can be derived as

$$\Psi(x) = \sum_l \Psi_l x^l = \left(1 - \frac{\Psi'(1)}{N}(1-x)\right)^N. \tag{2.8}$$

Using the asymptotic setting ($N, M \to \infty$), (2.8) becomes

$$\Psi(x) = e^{-\Psi'(1)(1-x)} = e^{-G\Lambda'(1)(1-x)}.$$

and using $\rho(x) = \Psi'(x)/\Psi'(1)$, we have

$$\rho(x) = e^{-G\Lambda'(1)(1-x)}. \tag{2.9}$$

As a last step, inserting (2.9) into (2.6) and (2.7), a recursive equation update becomes $p_i = 1 - e^{-G\Lambda'(1)\lambda(p_{i-1})}$.

It should be remarked that the asymptotic convergence analysis can be performed for any given user degree distribution $\Lambda(x)$ and channel load G. For the load values lower than a certain threshold, the probabilities p and q will converge to vanishing values and the packets will be recovered with probability close to 1. Above this threshold, the convergence of the probabilities p and q to small

Table 2.1: Optimized Distributions of IRSA with corresponding G^* values

User Degree Distributions $\Lambda(x)$	G^*
$\Lambda_4(x) = 0.5102x^2 + 0.4898x^4$	0.868
$\Lambda_5(x) = 0.5631x^2 + 0.0436x^3 + 0.3933x^5$	0.898
$\Lambda_6(x) = 0.5465x^2 + 0.1623x^3 + 0.2912x^6$	0.915
$\Lambda_8(x) = 0.5x^2 + 0.28x^3 + 0.22x^8$	0.938

values is not possible, i.e., some of the packets may be undecoded. Hence, we define G^* as the maximum achievable asymptotic load value where all users in the frame can be decoded successfully. We define the packet loss rate (PLR) as the percentage of packets not being decoded after the iterations are completed. Denoting the PLR by P_l, we can write $P_l = \Lambda(p_{i_{\max}})$ where $i_{\max}$ is the maximum number of iterations. Recalling the definition of the normalized throughput, we arrive at $T = G(1 - P_l)$.

The developed convergence analysis allows us to evaluate the system performance of a given user degree distribution $\Lambda(x)$. Hence, we look for the optimal degree distributions that provide the maximum G^* values using differential evolution. The optimized distributions of IRSA for different maximum number of replicas ($l_{\max}$), denoted by $\Lambda_{l_{\max}}(x)$, along with their corresponding channel load threshold values are presented in Table 2.1. We observe that the use of optimal irregular repetition rates is highly beneficial, and the throughput can be increased to 0.938 with $\Lambda_8(x)$ compared to 0.55 of CRDSA with $\Lambda_2(x) = x^2$. While allowing users to transmit their packets with multiple replicas contributes to the system performance, using a high number of replicas (more than 8) may not be practical due to the overhead caused by the stored location information of other replicas and the increased complexity of SIC iterations. Moreover, using a higher number of maximum allowed replicas increases the average repetition rates of the optimized distributions, which may deteriorate the energy efficiency of the system.

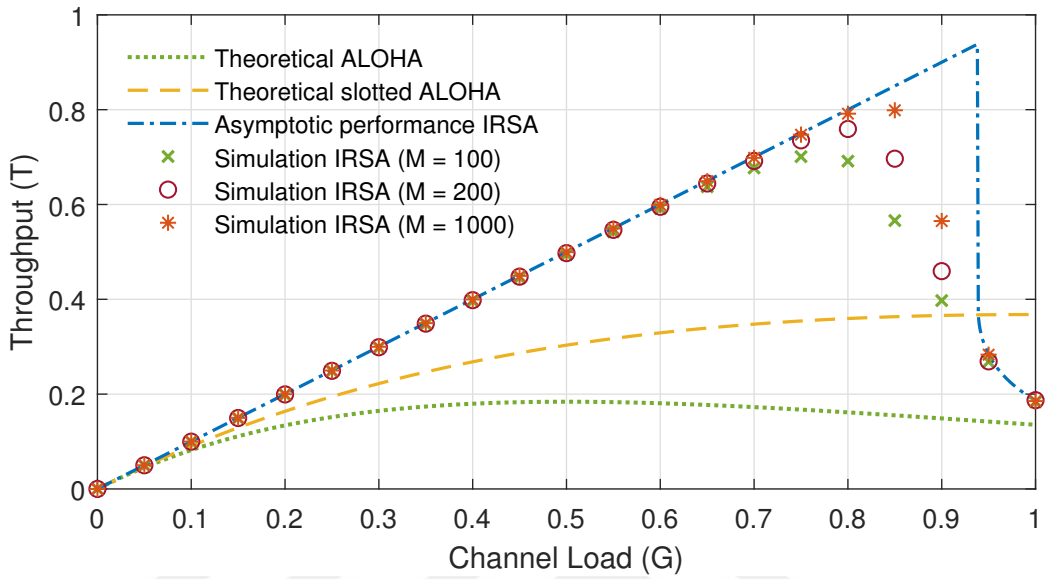

Figure 2.7: Asymptotic performance and finite length results of IRSA.

2.2.1.3 Numerical Examples

We now evaluate the performance of CRDSA and IRSA in both asymptotic and non-asymptotic (finite length) scenarios. As a first set of simulations, we only consider IRSA with distribution $\Lambda_8(x)$. We perform simulations over different finite frame lengths, i.e., $M = 100, 200, 1000$ by setting the iteration number to 20, i.e., $i_{\max} = 20$. In Fig. 2.7, the asymptotic throughput performance of $\Lambda_8(x)$ along with different finite frame lengths is depicted. It can be observed that the asymptotic throughput and channel load is almost identical due to the vanishing PLR up to G^*. The simulation results verify the results of the asymptotic convergence analysis as they approach to the asymptotic performance with anincreased number of slots per frame. Lower MAC frame durations result in a performance loss, however, it is still possible to obtain a good performance with moderate frame lengths, e.g., $M = 200$.

As a second set of simulations, we compare the performance of CRDSA and IRSA in Fig. 2.8. For simulations, we only consider the frame length of 200 slots with 20 iterations. We also provide the performance of ALOHA and slotted ALOHA. It is observed that optimized irregular repetition rates provide higher

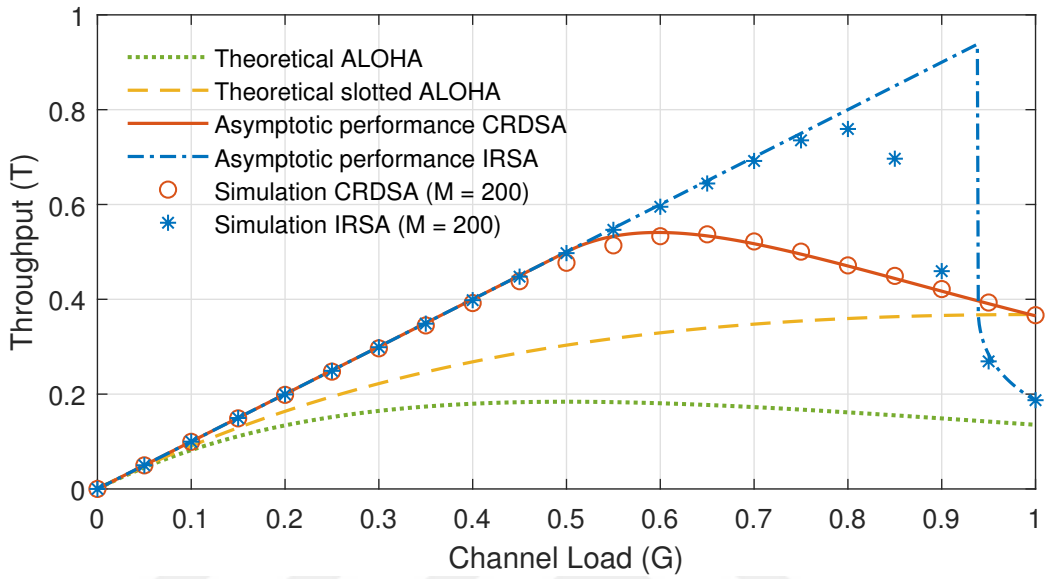

Figure 2.8: Asymptotic and finite length performance comparison of CRDSA and IRSA.

asymptotic throughput performance compared to the regular ones which is also valid for the finite length case. Moreover, the use of SIC with repetitions is highly advantageous in terms of throughput since both CRDSA and IRSA outperform ALOHA and slotted ALOHA.

2.2.2 Other Extensions

Coded slotted ALOHA (CSA) is a generalization of IRSA obtained by replacing the repetition codes with more powerful error correction codes (linear block codes) in [14]. In this scheme, packets are not simply repeated, instead they are encoded before the transmission, i.e., a packet is divided into k information segments and then encoded into n segments by an (n, k) linear block code. CSA retains all the advantages of IRSA and provides better results at the rate regime, $1/3 \leq R \leq 1/2$, while its advantage mostly vanish for the other regimes.

Many other extensions on the advanced RA schemes for different scenarios have also been studied in the literature. For example, in [15] the authors present

a frameless approach of IRSA and CSA in which an adaptive frame length is adopted, i.e., the frame is ended when the instantaneous throughput is maximized. In another related work, the authors in [16] show that the ideal truncated soliton distributions offer optimal performance in asymptotic settings. Another work [17] extends the density evolution analysis of IRSA to a fading channel model with a capture effect. The enhanced versions of CRDSA with packet power diversity over an additive white Gaussian noise (AWGN) channel and a collision channel are presented in [18, 19]. The work [20] presents an error floor analysis of CSA over packet erasure channels for finite frame lengths and the modified density evolution analysis of CSA over packet/slot erasure channels under the asymptotic setting is proposed in [21]. ZigZag decoding is first proposed in [22] to solve the hidden terminal problem for wireless local networks, while it is also used for slotted ALOHA and carrier sensing multiple access [23], frameless ALOHA [24], and coded slotted ALOHA [25]. The finite length analysis of frame asynchronous CSA and IRSA with tight approximations can be found in [26, 27].

We also draw attention to the line of studies on massive random access techniques starting with Polyanskiy in [28], where an information theoretic formulation of the problem is developed. Specifically, the random access scheme is modeled as follows: 1) the access mechanism is grant-free, 2) the users utilize the same codebook (unsourced access). In [28], achievability and converse bounds on the overall transmission rates for massive random access are derived. Practical coding schemes for this set-up with low-complexity coding approaches and more sophisticated LDPC coding schemes with SIC are presented in [29, 30]. In another related work [31], the authors consider ZigZag decoding for multiple access and also derive closed-form bounds on the achievable sum-rate of the system. This idea is based on performing interference cancellation with the received noisy signals and it is extendable to more than two users. With this approach, once the users are decoupled, single user codes can be adopted, hence by combining it with proper random access solutions, a simple and scalable solution for massive random access can be achieved.

2.3 Advanced Asynchronous RA Schemes

2.3.1 CRA

Contention resolution ALOHA (CRA) can be considered as a slot asynchronous counterpart of CRDSA [32]. In this scheme, the users still transmit their packets with regular repetition rates and the receiver resolves the collisions through SIC. The proposed scheme removes the stringent slot synchronization requirement among users, however frame level synchronization is still adopted. The slot asynchronism allows for lower complexity transmitters and relaxes the timing requirements.

CRA also benefits from forward error correction (FEC) codes to resolve the packets even under collision on the physical layer (different from CRDSA). This approach uses signal-to-interference noise ratio (SINR) based decoding and it is assumed that a packet replica can be decoded if the amount of collision is under the determined threshold which is approximated by an information theoretic bound. It is shown that CRA can provide comparable or even better performance compared to CRDSA using FEC codes by taking the advantage of partial collisions due to the asynchronism. However, this advantage disappears when FEC codes are not utilized.

2.3.2 ECRA

Enhanced CRA (ECRA), first proposed in [33], improves the performance of CRA by a two-step decoding procedure. In the first step, the receiver decodes the packets under the determined SINR threshold, and removes their corresponding interference from the MAC frame iteratively as in CRA. Differently, in the second step, the receiver tries to combine parts of the replicas with minimum interference (or, no interference if possible) to obtain a new combined packet with the lowest possible interference. This additional procedure guarantees that ECRA outperforms CRA, however, this performance improvement comes at a

cost of higher decoding complexity.

The second version of ECRA [34] removes the frame synchronization requirement as well, hence the scheme is fully asynchronous. In this version, different combining techniques, e.g., selection and maximal-ratio combining, are used to obtain a new combined packet over a block interference channel model [35]. Moreover, a tight approximation of PLR for low channel loads is derived. A performance evaluation of ECRA in comparison with CRA and CRDSA is performed in [34] as well.

2.3.3 ACRDA

Asynchronous contention resolution diversity ALOHA (ACRDA) is a fully asynchronous adaptation of CRDSA by removing both frame- and slot-level synchronization with reduced complexity and lower transmission delay. Users have their own local frames for transmissions since there are no common MAC frames. An approximate analysis of the scheme is performed using the most frequently occurring loops for PLR calculation. This scheme also utilizes FEC codes to resolve the collisions similar to CRA and ECRA. ACRDA provides comparable throughputs and lower PLR values compared to CRDSA taking advantage of full asynchronism.

2.4 EH RA Schemes

Regarding ALOHA based schemes adopting energy harvesting nodes, in [36], the authors study the effect of system parameters, i.e., contention window size, packet and energy arrival rates, utilizing a proposed closed queuing network mathematical model in a slotted ALOHA based network with wireless energy harvesting nodes. They also consider the sum throughput maximization of the energy harvesting capable slotted ALOHA for static and dynamic transmission policies with Markov chain and decision process in [37]. The stability region of two-node slotted

ALOHA system with nodes having different energy harvesting rates and activation probabilities is investigated in [38]. They also examine the effect of finite battery capacity on the achievable stability region. In [39], the authors present the energy harvesting aware design and analysis of different MAC protocols, e.g., TDMA, framed ALOHA (FA) and dynamic framed ALOHA (DFA), in detail. They study the challenges posed by the uncertain amount of harvested energy from the environment. Another line of work [40] studies the approximate capacity of the energy harvesting channel with a finite-sized battery and other related works on different MAC protocols with energy harvesting capable nodes can be found in [41–43]. A comprehensive study on the area of energy harvesting wireless communications can be found in [44].

As a more closely related approach to the development in this thesis, energy harvesting irregular repetition slotted ALOHA (EH-IRSA) scheme is first proposed by accommodating energy harvesting user nodes with a unit-sized battery in [45], and then, the scheme is extended to the case of finite-sized battery equipped nodes in [46]. The transmission of replicas take place only if there is a sufficient amount of harvested energy in the user battery. Hence, a user may not be able to transmit some of its planned replicas. The stochastic nature of energy availability necessitates a renewed design and analysis. With this motivation, the authors propose a scheme as a modification of IRSA. Specifically, since a user may not be able to transmit the determined number of replicas due to the lack of energy, the actual (effective) repetition distribution $\tilde{\Lambda}(x)$ of the replicas being transmitted is different from the chosen initial distribution $\Lambda(x)$. The authors compute $\tilde{\Lambda}(x)$ for given system and EH parameters, and perform the asymptotic convergence analysis in a similar fashion to that of IRSA. They also obtain the optimized repetition distributions, and show that the new degree distributions for the energy harvesting scenario perform remarkably better than the regular and optimized irregular distributions of CRDSA and IRSA for both asymptotic and practical scenarios.

2.5 Chapter Summary

In this chapter, we first present basic RA protocols to supply some background information. We then review the advanced synchronous RA schemes and present the convergence analysis of CRDSA and IRSA with performance comparisons. We also review the related asynchronous schemes. We present the literature review on energy harvesting ALOHA based RA protocols by remarking EH-IRSA.

Table 2.2: Main features of related ALOHA based advanced RA schemes

RA Scheme	Frame Asyncronous	Slot Asyncronous	Irregular Repetition Rates	Main Feature
CRDSA [3]	✗	✗	✗	Frame and slot synchronous scheme with regular repetition rates
IRSA [12]	✗	✗	✓	Generalization of CRDSA with irregular repetition rates
EH-IRSA [46]	✗	✗	✓	Adaptation of IRSA with energy harvesting nodes
CRA [32]	✗	✓	✗	Slot asynchronous counterpart of CRDSA
ACRDA [47]	✓	✓	✗	Fully asynchronous adaptation of CRDSA
ECRA [34]	✓	✓	✗	Frame asynchronous enhanced version of CRA with combining techniques
IRA [5]	✗	✓	✓	Asynchronous RA scheme with irregular repetition rates
IRARC [5]	✗	✓	✓	IRA with replica concatenation
EH-(IRA-IRARC)	✓	✓	✓	IRA and IRARC with energy harvesting nodes
IRA-PLD [6]	✗	✓	✓	Extension of IRA with different packet lengths

We provide a table to summarize the related advanced RA schemes along with their main features in Table 2.2. We emphasize that all the listed advanced RA schemes provide remarkable performance improvements over ALOHA, slotted ALOHA and diversity slotted ALOHA (DSA).

Chapter 3

CRA and IRA with Replica Concatenation

In this chapter, we consider an asynchronous random access scheme called IRA as a generalization of CRA with varying repetitions. We present an asymptotic performance analysis of CRA and IRA on the collision channel for regular and irregular repetition rates. We also propose an improvement to them by merging the clean parts of packet replicas in partial collisions, and extend our analysis to this scenario as well. Specific designs of repetition distributions based on the new analysis show that the optimized solutions of IRSA perform well in both IRA and the enhanced scheme, and they considerably outperform the regular repetition distributions.

The chapter is organized as follows. In Section 3.1, we describe the system model. The asymptotic analyses of CRA and IRA are developed in Section 3.2. In Section 3.3, the analysis is extended to CRA/IRA with two replica concatenation. Optimized repetition distributions and numerical results are given in Section 3.4. Finally, Section 3.5 presents our summary.

3.1 System Model

In this section, we first present the system model of the asynchronous RA schemes under consideration, namely, IRA and IRARC. We then describe the channel model and SIC mechanism.

3.1.1 RA Scheme

We consider an asynchronous random access scheme with the motivation that such schemes can allow users to transmit their packets at arbitrary time instants to a single receiver within a MAC frame, and hence, they remove the stringent slot synchronization requirement for users. Each MAC frame has equal duration denoted by T_f and it is the same for all users. Users transmit a packet upon its arrival via copies of its packets, called as replicas, within a frame. We assume that a user can have only one packet to be transmitted within a frame. All the packets and their copies have an equal duration denoted by τ. The transmission time of the replicas are uniformly distributed over the duration of a frame. The packet replicas include the preamble sequences for the packet detection and channel estimation. Also, each packet replica contains the position information of other replicas inside the frame relative to its own location, e.g., with a pre-determined quantization of the time differences. We note that such a quantization requires detection of the packets using the common preamble sequences.

In our model, the users are sporadically activated with probability π at the beginning of each frame. The activation probability is independent of users and frames. Active users transmit their packets with a certain number of replicas, called as repetition rate, at different frames. The repetition rate might be regular as in CRA with all active users transmitting a fixed number of replicas, or it can be drawn from a certain probability mass function (PMF) for each user in each frame as in IRSA. The total number of users, including both active and inactive users, is denoted by N_t. The number of active users, N_a, follows a Binomial distribution, and the expected number of active users is denoted by N,

i.e., $N = \mathbb{E}[N_a] = \pi N_t$. Even though the number of users is massive, because of the sporadic nature of the users, the active number of users at a certain time is limited, $\pi \ll 1$. We define the channel (normalized) load as the expected number of active users within the duration τ, i.e.,

$$G = \frac{\mathbb{E}[N_a] \cdot \tau}{T_f} = \frac{N \cdot \tau}{T_f}. \tag{3.1}$$

We also define the load generated by multiple packet replicas, i.e., the physical load, denoted as μ, as the expected number of packet replicas in an interval of length τ, i.e., $\mu = d_{avg} \cdot G$ where d_{avg} is the expected number of packet replicas per user [1].

Finally, we define the packet loss rate (PLR), denoted by P_l, as the percentage of the packets (on average) that are not decoded at the receiver after all SIC iterations are completed, and the normalized throughput, T, as the expected number of successfully decoded packets in an interval of length τ, i.e., $T = (1 - P_l)G$.

3.1.2 Channel Model and Decoding Process

We adopt a multiple access collision channel, as typically considered in the analysis of RA schemes [12], where the receiver is able to detect whether a packet experiences collision or not. Collisions are destructive (unless the interference is removed), and if a packet experiences interference, it cannot be resolved correctly. Otherwise, it is always decoded successfully. We also assume that the receiver can distinguish the clean parts of the replicas for the replica concatenation scenario.

The receiver applies the SIC for IRA over MAC frames. In each frame, SIC iterations (also referred to as iterations) are applied as follows: 1) The receiver detects the packet replicas and estimates the channel information, in particular, the symbol timing, carrier frequency and phase, using the preamble and payload

[1] We note that G is defined scaling the expected number of active users by τ/T_f but not to replicas. G and μ are defined for the duration of τ since our analysis is performed with respect to this duration.

symbols. 2) The packets that are not in a collision are decoded. 3) The symbols of the decoded packets are regenerated by re-encoding and re-modulating the payload information and signaling bits. 4) With the help of channel and location information, the regenerated packets are used to remove interference of the other replicas of that packet from the resolution window. We need to remark that as discussed in [3] and [47], the symbol timing and carrier frequency are identical for the replicas that belong to the same packet, however, this is not the case for carrier phase since it is uncorrelated between different replicas. The phase needs to be re-estimated for the other replicas which can be performed with correlation based techniques. The SIC iterations are applied until there is no collision-free replica in the frame or the maximum number of iterations reached. After that, the SIC mechanism is repeated again for the new frame. Throughout the chapter, we assume that channel parameters' estimates are perfect, and hence, interference cancellation is ideal. A more detailed discussion about imperfect (actual) SIC and parameter estimation can be found in [3] and [12].

For the enhanced scheme of IRARC, the receiver needs to concatenate the replicas with some clean portion to obtain a complete clean packet. We assume that the receiver can still detect a packet through the preamble sequence even under collision [2] and discriminate the clean parts of a packet using the in-phase and quadrature binary (± 1) payload symbols. Next, the receiver can estimate the channel parameters with the preamble sequence and interference free payload symbols, and obtain a complete clean packet. Lastly, the SIC mechanism can take place similar to IRA with this clean packet. The proposed enhancement brings additional complexity and may increase decoding delay. However, the replica concatenation is only employed when there is no clean packet remaining in the frame (the SIC mechanism of IRA cannot progress any further). Hence, the replica concatenation is an additional process to SIC mechanism of IRA and the complexity of the enhancement is mostly limited. The additional complexity due to the replica concatenation is only to detect the clean symbols of the packets and the concatenation of these symbols which is not computationally demanding.

[2] As pointed out in [3] and [47], preamble collision is highly unlikely and with a small frequency or time off-set, the preambles can be identified surely. Alternatively, similar to ZigZag decoding, multiple preambles can be located on both ends of a packet.

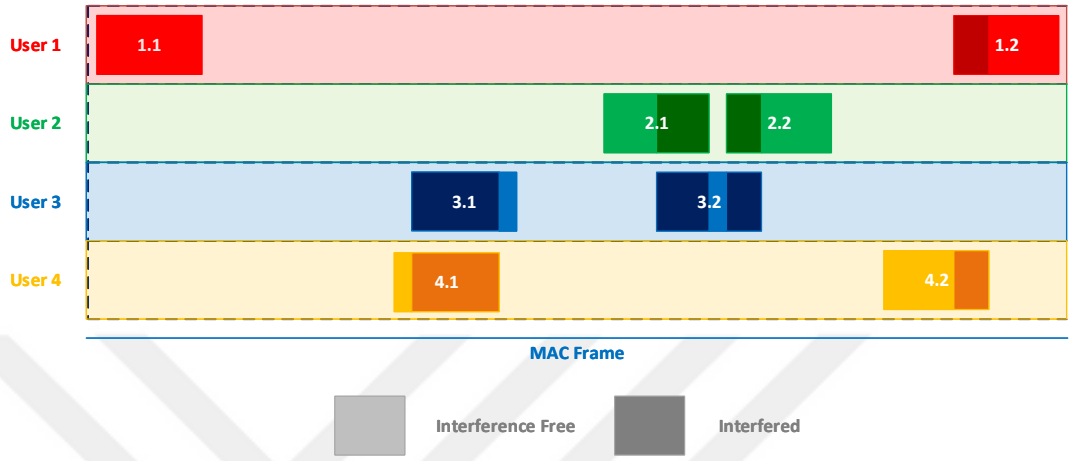

Figure 3.1: An illustration of MAC frame description and SIC procedure of IRA.

We also limit the number of replicas to be used in concatenation to 2 to lower the complexity.

An exemplary scenario of an ideal SIC procedure for IRA is illustrated at Fig. 3.1 which depicts 4 active users transmitting 2 replicas within a MAC frame. First, it can be seen that the only interference free replica belongs to user 1. The packets are decoded with the following SIC iterations: *Iteration I)* The receiver detects the interference-free replica and decodes the packet of user 1. Exploiting SIC, the interference of the second replica of user 1 is extracted from the received signal. *Iteration II)* User 4's second replica is now interference-free and can be decoded correctly. The replicas of user 4 are cleaned from the received signal. *Iteration III)* User 3's packet can be decoded successfully and its interference is removed. *Iteration IV)* User 2 is the only remaining user in the system and is also decoded successfully.

3.2 Asymptotic Analysis of CRA/IRA

In this section, we present an analysis for CRA and IRA. We consider the asymptotic setting [3] $(N, T_f \to \infty)$ while keeping the channel load G, activation probability π and packet duration τ constant . In this setting, the replicas become statistically independent from each other, and they have identical statistics (including the success and failure probabilities through the SIC iterations) allowing us to examine each replica separately. Hence, determining the behavior of a sample replica is sufficient to analyze the entire scheme.

3.2.1 Regular Repetition Rates (CRA)

In this case, each user's packet is transmitted via d replicas as illustrated in Fig. 3.2. Consider a specific packet and one of its replicas. We denote the probability of that replica not being resolved during iteration i by p_i. We also define q_i as the probability of the other replicas of that packet not being resolved at the previous iteration $(i-1)$. A replica is unknown only if identical $d-1$ other replicas are not resolved at the previous iteration, i.e., $q_i = p_{i-1}^{d-1}$. Similarly, a replica cannot be decoded during iteration i if at least one of the l interfering packets are not subtracted from the received signal, i.e., $p_i = 1-(1-q_i)^l$. To clarify, we refer to the Fig. 3.2. The packet replica 2.2 carries erasure at the current iteration if all of the remaining replicas are not decoded at the previous one. Similarly, the sample replica 1.2 is erasure free only if all the replica arrivals inside the vulnerable period are known. Using the relationships, we can write the probability of not being resolved recursively as $p_i = 1-(1-p_{i-1}^{d-1})^l$. Throughout the analysis, we will refer to μ_i as the remaining (unresolved) load at iteration i, i.e., $\mu_i = \mu q_i$.

We now compute the probability of l packet arrivals inside the vulnerable period of the sample replica, i.e., the replicas that arrive in a specific interval

[3] The asymptotic setting allows us to develop tractable mathematical tools for the repetition rate optimization rather than focusing on the fine-tuned performance of the finite length scenario. The finite length analysis of advanced RA schemes differ from the asymptotic analysis and they are extremely challenging. Some works along this direction are reported in [26, 27].

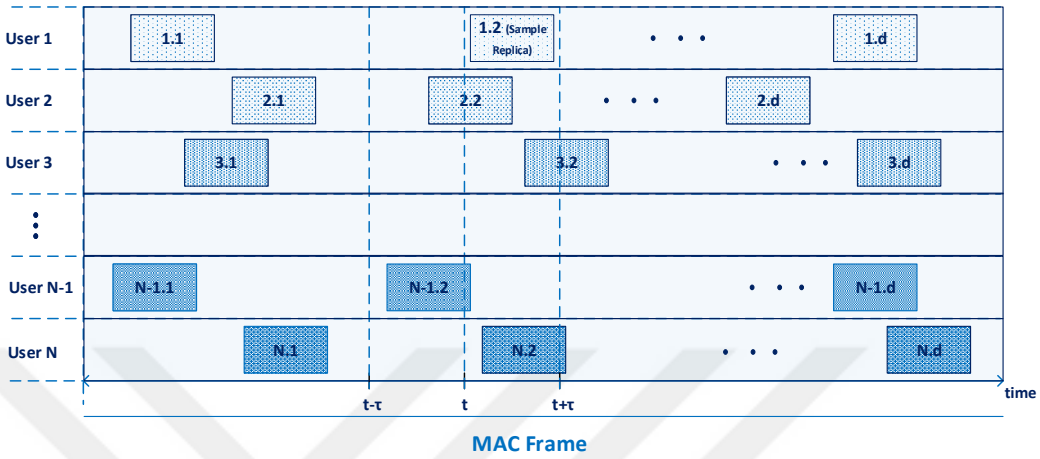

Figure 3.2: A sample from MAC frame of CRA with N active users and d replicas.

of length of 2τ collide with the reference replica. A user transmits a replica inside this vulnerable period with a probability of $2\tau d/T_f$. Hence, we can write the probability of l interfering replica arrivals colliding with the sample replica denoted by ρ_l using the binomial distribution as

$$\rho_l = \binom{N}{l}\left(\frac{2\tau d}{T_f}\right)^l\left(1-\frac{2\tau d}{T_f}\right)^{N-l}.$$

Using the asymptotic setting, letting $(N, T_f \to \infty)$, ρ_l becomes a Poisson random variable with parameter $2dG$ (2μ), i.e.,

$$\rho_l = e^{-2dG}\frac{(2dG)^l}{l!} = e^{-2\mu}\frac{(2\mu)^l}{l!}.$$

At the first iteration, none of the replicas are resolved (prior to the start of SIC, $p_0 = q_0 = 1$), hence, for successful decoding of a chosen replica, there should not be any replica arrival inside the interval of length 2τ, i.e.,

$$p_1 = 1 - \rho_0 = 1 - e^{-2\mu}.$$

Consider a specific packet replica after the execution of the first iteration. For the replica to be resolved, there should not be any unresolved replicas inside its vulnerable period. Hence, the remaining load at the second iteration, which is the expected arrival rate of unresolved replicas with respect to the specific replica, can be denoted as $\mu_2 = \mu q_2 = \mu p_1^{d-1}$. The load is scaled with the probability of a packet not being resolved in the first iteration which is only possible if the remaining $(d-1)$ replicas are not resolved. Hence, by using the remaining load, we write $p_2 = 1 - e^{-2\mu_2}$.

To clarify, we now compute p_2 for a specific replica explicitly. With l replicas inside its vulnerable period, 2τ, either there are no unresolved replicas, i.e., all the l replicas are decoded at iteration 1, and the specific replica can be resolved, or there is at least one unresolved replica and the specific replica cannot be resolved. Since each of the l replicas has a probability of $(1-q_2)$ being resolved, the probability of all of the l replicas not being decoded is written as $1-(1-q_2)^l$. Thus, by applying the total probability theorem, we obtain

$$p_2 = \sum_{l=0}^{\infty} \frac{e^{-2\mu}(2\mu)^l}{l!}\big(1-(1-q_2)^l\big) = 1 - e^{-2\mu_2}.$$

After describing the SIC procedure for iteration 1 and 2, we now write p_i for an arbitrary iteration i. Recall that we have the recursive relationship $p_i = 1-(1-p_{i-1}^{d-1})^l$, which allows us to calculate the non-resolvability probability at the i-th iteration in terms of the $(i-1)$-st one. Hence, one can obtain p_i by averaging over the l replica arrival probability, ρ_l, i.e.,

$$p_i = \sum_{l=0}^{\infty} \rho_l\big(1-(1-p_{i-1}^{d-1})^l\big) = 1 - e^{-2\mu p_{i-1}^{d-1}} = 1 - e^{-2\mu_i}. \tag{3.2}$$

3.2.2 Irregular Repetition Rates (IRA)

We now consider the scenario where the number of replicas are drawn from an arbitrary PMF, instead of being picked as constant d. We define $\Lambda(x)$ as the user

degree distribution, i.e.,

$$\Lambda(x) \triangleq \sum_{d=1}^{d_{\max}} \Lambda_d x^d,$$

where Λ_d denotes the probability of a user transmitting d replicas and $d_{\max}$ is the maximum number of replicas. Average packet repetition rate can be found as $\Lambda'(1) = \sum_d d\Lambda_d$, and $\mu = \Lambda'(1)G$.

In order to extend the analysis in the previous subsection to this case, we again examine the receiver operations on a specific packet replica. We first compute the probability of a randomly selected replica belonging to a user with a repetition rate of d as

$$\lambda_d = \frac{d\Lambda_d}{\sum_{d=1}^{d_{\max}} d\Lambda_d}.$$

We also define the replica degree distribution in polynomial form, $\lambda(x)$, as

$$\lambda(x) \triangleq \sum_{d=1}^{d_{\max}} \lambda_d x^{d-1} \text{ where } \lambda(x) = \frac{\Lambda'(x)}{\Lambda'(1)}.$$

We need to update the definition of q_i, i.e., $q_i = p_{i-1}^{d-1}$, since active users might have different replica numbers. Therefore, we average over the replica degree distribution to obtain q_i as

$$q_i = \sum_{d=1}^{d_{\max}} \lambda_d \cdot p_{i-1}^{d-1} = \lambda(p_{i-1}),$$

The remaining load can also be expressed in terms of G similar to CRA as $\mu_i = \Lambda'(1)G\lambda(p_{i-1})$, and we can rewrite p_i in a generic form as follows

$$p_i = 1 - e^{-2\mu\lambda(p_{i-1})} = 1 - e^{-2\mu_i}. \tag{3.3}$$

Connection to PLR: Recalling the definitions of the packet loss rate and the

normalized throughput, we write $P_l = \Lambda(p_{i_{\max}})$ and $T = (1 - P_l)G$. We note that after all iterations completed, $p_{i_{\max}}$ is obtained representing the non-resolvability probability of a replica. For a packet (user) to be lost, all replicas should be unresolved, i.e., for a user with d replicas, the probability of its packet not being decoded is $p_{i_{\max}}^d$. Since user degree distribution is a polynomial representation of number of replicas, PLR can be written as $P_l = \Lambda(p_{i_{\max}})$ averaging over the user degree distribution. We emphasize that these expressions are valid for both regular and irregular repetition scenarios. In the rest of the thesis, we will continue only with IRA, as its analysis is more generic, and it covers the case of CRA as well.

We also note that the provided analysis is amenable to different extensions although it is mainly developed for the destructive channel model. For instance, a packet can still be decoded with some level of interference relaxing the strict condition of collision channel with the use of FEC codes. To extend the analysis for such a scenario, the probability of decoding the colliding packets needs to be derived and incorporated into the analysis in a similar way to the works extending IRSA for different channel conditions and scenarios (e.g., [17, 21]). For instance, [32] adopts an SINR based decoding criterion which can be covered by our analysis by redefining the condition for successful recovery.

3.3 IRA with Two Replica Concatenation (IRARC)

We now consider an extended version of IRA with SIC by concatenation of two overlapped replicas of a packet to build an interference free packet from the clean parts of collided replicas. Our aim is to benefit from the partial collisions caused by asynchronism. We limit the number of replicas whose clean parts are combined to only two in order to keep the algorithm simple and examine the effect of this simplification in the numerical results section.

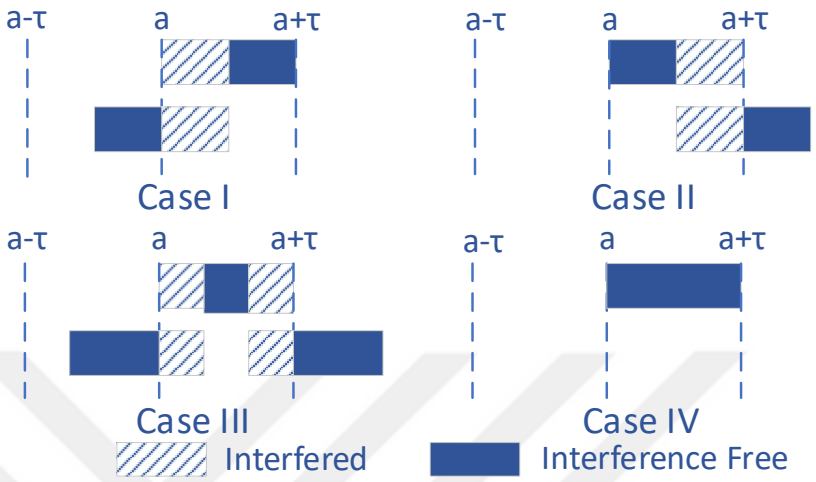

Figure 3.3: Possible collision scenarios for a packet replica with some clean part.

3.3.1 Preliminaries

There are four possible cases that a packet replica (with some clean portion) may encounter as illustrated in Fig. 3.3. To explain, we divide the vulnerable period of the replica under consideration into two equal length intervals as $(a-\tau, a)$ and $(a, a+\tau)$ (where a is the transmission start time of the packet). In case I, the packet is collided only from the left-hand side meaning that there are colliding replicas starting in $(a-\tau, a)$ only. A similar argument holds for the packet that is only collided from the right-hand side (case II). In case III, the packet is collided from both sides at the same time. In addition to these three cases, completely interference free packets constitute case IV.

We now determine the amount of collisions from the left-hand and right-hand sides. We define two events C_k^- and C_l^+ to represent the events of having k and l colliding replica arrivals in the intervals $(a-\tau, a)$ and $(a, a+\tau)$, respectively. Therefore,

$$\Pr\{C_k^-\} = \frac{e^{-\mu}\mu^k}{k!}, \quad \Pr\{C_l^+\} = \frac{e^{-\mu}\mu^l}{l!},$$

as the arrivals follow a Poisson process with intensity μ. For Poisson arrivals,

conditioned on the number of arrivals in a given interval, the arrival time of the replicas are independent and identically distributed (i.i.d.) uniform random variables within their respective intervals. Hence, conditioning on the events C_k^- and C_l^+, we denote the arrival times of the replicas in $(a-\tau, a)$ and $(a, a+\tau)$ as $U_1^-, U_2^-, ..., U_k^-$ and $U_1^+, U_2^+, ..., U_l^+$, respectively, and take $\tau = 1$ for simplicity of notation while a can be any arbitrary value. We define random variables X, $Y \in [0, 1]$ to denote the maximum amount of collision from the left-hand and the right-hand sides, i.e.,

$$X = \max_{1 \le i \le k} U_i^-, \quad Y = 1 - \min_{1 \le j \le l} U_j^+.$$

The cumulative distribution function (CDF) and probability density function (PDF) of X and Y conditioned on C_k^- and C_l^+ are: $F_X(x \mid C_k^-) = x^k$, $F_Y(y \mid C_l^+) = y^l$, $f_X(x \mid C_k^-) = kx^{k-1}$, and $f_Y(y \mid C_l^+) = ly^{l-1}$, $x, y \in [0, 1]$. Note that conditional PDFs and CDFs of X and Y are identical, and by using the total probability theorem, we can write

$$F_X(x) = \sum_{k=0}^{\infty} \Pr\{C_k^-\} F_X(x \mid C_k^-) = e^{-\mu(1-x)}, \text{ for } x \in [0, 1].$$

Hence $f_X(x) = e^{-\mu}\delta(x) + \mu e^{-\mu(1-x)}(u(x) - u(x-1))$ where $u(x)$ is the unit step function, i.e., X is a mixed random variable with a mass point at $x = 0$. Note that for the asymptotic analysis, we utilize the continuous part of X. Hence, the conditional PDF and CDF defined as $f_{X|R}(x) = \frac{\mu e^{-\mu(1-x)}}{1-e^{-\mu}}$ and $F_{X|R}(x) = \frac{e^{-\mu(1-x)} - e^{-\mu}}{1-e^{-\mu}}$, $x \in (0, 1]$, with event $R = \{X \neq 0\}$ are also needed.

3.3.2 Asymptotic Analysis

We now provide an asymptotic analysis for IRA with two replica concatenation. Noting that case IV packets are not included in the analysis, we only need the additional resolvability probability (due to the packets that cannot be resolved by IRA alone) to perform the analysis. Hence, the objective is to find the successful

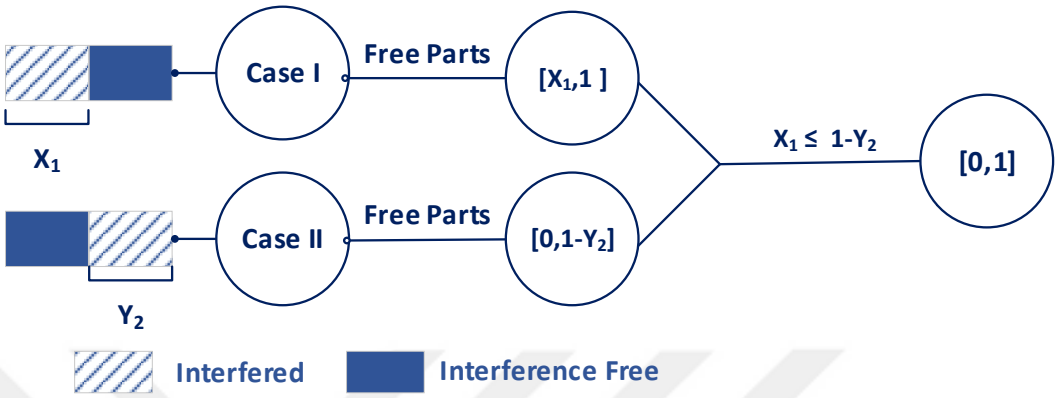

Figure 3.4: A concatenation example with two replicas belonging to the cases I and II.

concatenation probability of the unresolved packets using the clean portions of colliding replicas. Note that using only two partially colliding replicas for concatenation simplifies our analysis as case III replicas cannot be used to recover a packet in this scenario, i.e., utilization of case-III replicas require at least three replicas to be combined since they have collisions from both sides. Thus, these two replicas need to have collisions only from the left- or the right-hand sides (cases I-II), respectively. Consider two replicas which belong to case I and II, respectively, as depicted in Fig. 3.4. Let X_1 and Y_2 denote the amount of collisions from the left-hand and right-hand sides of the two replicas, respectively. Free parts of these replicas are in the intervals $[X_1, 1]$ and $[0, 1 - Y_2]$. The successful recovery, i.e., $[0, 1] = [X_1, 1] \cup [0, 1 - Y_2]$, is possible only if $X_1 \leqslant 1 - Y_2$.

Let us consider a user with d packet replicas. We denote the number of replicas experiencing case-I, case-II and case-III by k, n and $d - n - k$ respectively. The selection of replicas can be made in $\binom{d}{n,k} = \frac{d!}{n!k!(d-n-k)!}$ different ways. With $\xi(d, n, k)$ denoting the probability of k, n and $d - n - k$ packets belonging to

case-I, case-II and case-III, respectively, we write

$$\begin{aligned}\xi(d,n,k) &= \binom{d}{n,k}\prod_{l=1}^{k}\underbrace{\Pr\{X_l\neq 0, Y_l=0\}}_{\text{case-I}}\cdot\prod_{m=k+1}^{n+k}\underbrace{\Pr\{X_m=0, Y_m\neq 0\}}_{\text{case-II}}\\ &\quad\cdot\prod_{s=n+k+1}^{d}\underbrace{\Pr\{X_s\neq 0, Y_s\neq 0\}}_{\text{case-III}}\\ &= \binom{d}{n,k}\prod_{l=1}^{k}\Pr\{Y_l=0\}\cdot\Pr\{T_k\}\cdot\prod_{m=k+1}^{n+k}\Pr\{X_m=0\}\cdot\Pr\{S_n\}\\ &\quad\cdot\prod_{s=n+k+1}^{d}\Pr\{X_s\neq 0, Y_s\neq 0\}\end{aligned} \tag{3.4}$$

where $T_k = \bigcap_{l=1}^{k}\{X_l \neq 0\}$ and $S_n = \bigcap_{m=1}^{n}\{Y_{k+l} \neq 0\}$. We note that the definitions of these events will be utilized to derive the probability of conditional successful recovery.

For the successful concatenation probability, we first search for the replica with the largest clean part from the left-hand side that belongs to case-II, and then look for a second replica with the smallest collided part from the left-hand from case-I that we can concatenate with the first one. The amount of the smallest collided part from the left-hand side among the k replicas is denoted by W_k, i.e., $W_k = \min\limits_{1\leq l\leq k}(X_l)$ and the amount of the largest clean part from the left-hand side among the n replicas is denoted by Z_n, i.e., $Z_n = \max\limits_{1\leq m\leq n}(1-Y_{k+l})$. Clearly, a successful recovery is possible, as we mentioned earlier, only if $W_k \leqslant Z_n$.

We define $\zeta(d,n,k)$ as the probability of successful concatenation for a user with d repetitions given k case-I, n case-II and $d-n-k$ case-III packets. Then, $\zeta(d,n,k)$ can be written in terms of $\xi(d,n,k)$ by inserting the successful recovery condition ($W_k \leqslant Z_n$) into (3.4):

$$\zeta(d,n,k) = \xi(d,n,k)\cdot\Pr\{W_k \leqslant Z_n \mid T_k, S_n\}. \tag{3.5}$$

As a next step, we need to calculate the probability $\Pr\{W_k \leqslant Z_n \mid T_k, S_n\}$. Note that the probability of T_k and S_n are $\Pr\{T_k\} = (1-e^{-\mu})^k$ and $\Pr\{S_n\} =$

$(1-e^{-\mu})^n$. We determine the conditional CDF of W_k and Z_n conditioned on the events T_k and S_n as

$$F_{W_k|T_k}(w) = 1 - \frac{(1-e^{-\mu(1-w)})^k}{(1-e^{-\mu})^k},\ F_{Z_n|S_n}(z) = \frac{(1-e^{-\mu z})^n}{(1-e^{-\mu})^n},$$

for $w, z \in (0,1]$. Using these, we obtain

$$\Pr\{W_k \leqslant Z_n \mid T_k, S_n\} = 1 - \frac{n}{(1-e^{-\mu})^{n+k}} \int_0^{1-e^{-\mu}} \left(1 - \frac{e^{-\mu}}{1-u}\right)^k u^{n-1}\, du, \quad (3.6)$$

by simplifying the integral $\int_0^1 F_{W_k|T_k}(z) f_{Z_n|S_n}(z)\, dz$. The integral in (3.6) can be written in terms of the Appell hypergeometric function ($F_1(a; b_1, b_2; c; x, y)$) [4] [48], i.e.,

$$\int_0^{1-e^{-\mu}} \left(1 - \frac{e^{-\mu}}{1-u}\right)^k u^{n-1}\, du = \frac{(1-e^{-\mu})^{(n+k)}}{n} F_1(n; k, -k; n+1; 1-e^{-\mu}, 1),$$

hence

$$\Pr\{W_k \leqslant Z_n \mid T_k, S_n\} = 1 - F_1(n; k, -k; n+1; 1-e^{-\mu}, 1). \quad (3.7)$$

We can then rewrite $\zeta(d, n, k)$ by plugging (3.7) into (3.5) as

$$\zeta(d, n, k) = \binom{d}{n, k} e^{-\mu(n+k)} (1-e^{-\mu})^{(2d-n-k)} (1 - F_1(n; k, -k; n+1; 1-e^{-\mu}, 1)).$$

We also define $\zeta(d)$ as the total successful concatenation probability of a user with d replicas in terms of $\zeta(d, n, k)$ by summing over all possible n and k values, i.e.,

$$\zeta(d) = \sum_{n=1}^{d-1} \sum_{k=1}^{d-n} \zeta(d, n, k).$$

[4] The Appell hypergeometric function is defined in a generic form as, $F_1(a; b_1, b_2; c; x, y) = \sum_{m=0}^{\infty} \sum_{n=0}^{\infty} \left(\frac{(a)_{m+n} (b_1)_m (b_2)_n}{m! n! (c)_{m+n}}\right) (x^m y^n)$. The term $(x)_n$ is the Pochhammer symbol given by $(x)_n = \frac{\Gamma(x+n)}{\Gamma(x)}$.

To utilize these derivations in the analysis, we finally update the generic load μ with the remaining load at iteration i, μ_i. For simplicity, we add a subscript i to $\zeta(.)$, for any function ζ computed for the load μ_i. We also need to define the probability of successful concatenation with respect to an unknown replica for iteration updates, denoted by $\bar{\zeta}_i(d)$, which can be written in terms of $\zeta_i(d)$ as $\bar{\zeta}_i(d) = \frac{\zeta_i(d)}{p_i}$ (where p_i stands for the failure probability of a packet).

We then specify ζ_i and $\bar{\zeta}_i$ as the expected success recovery probabilities for irregular repetition rates obtained by averaging $\zeta(d)_i$ and $\bar{\zeta}_i$ over the user and replica degree probabilities, Λ_d and λ_d, as

$$\zeta_i = \sum_{d=1}^{d_{\max}} \Lambda_d \cdot \zeta_i(d), \quad \bar{\zeta}_i = \sum_{d=1}^{d_{\max}} \lambda_d \cdot \bar{\zeta}_i(d).$$

As the last step, we revise the remaining load defined in Section III as $\mu_i = \mu\lambda(p_{i-1})$. Since, by performing replica concatenation, the receiver is now able to decode some additional packets among the remaining ones with probability $\bar{\zeta}_{i-1}$ at iteration $i-1$, the remaining load is updated as $\mu(\lambda(q_{i-1}) - \bar{\zeta}_{i-1})$ for the i-th iteration. Finally, the PLR updated as $P_l = \Lambda(p_{i_{\max}}) - \zeta_{i_{\max}}$ and $T = (1 - P_l)G$ in a similar manner to IRA.

3.4 Numerical Results

In this section, we illustrate the asymptotic and finite-length simulation results of IRA and IRARC schemes with the optimized repetition distributions. We utilize the developed asymptotic tools in Sections III and IV which enable us to determine the asymptotic P_l and normalized throughput of IRA/IRARC for any given user degree distribution, $\Lambda(x)$, and search for the optimal distributions over possible load values. We aim at maximizing the asymptotic channel load, G^*, providing a vanishing P_l, for a given maximum repetition rate by using differential evolution [13]. We define the maximum achievable asymptotic throughput T^* as the corresponding throughput value for G^*, specifically, $T^* = G^*$ in this

Table 3.1: Asymptotic Performance of Distributions

User Degree Distributions $\Lambda(x)$	CRDSA/IRSA(G^*)	CRA/IRA(G^*)	CRARC/IRARC(G^*)
$\Lambda_2(x) = x^2$	0.541	0.271	0.344
$\Lambda_4(x) = 0.5102x^2 + 0.4898x^4$	0.868	0.434	0.543
$\Lambda_5(x) = 0.5631x^2 + 0.0436x^3 + 0.3933x^5$	0.898	0.449	0.561
$\Lambda_6(x) = 0.5465x^2 + 0.1623x^3 + 0.2912x^6$	0.915	0.457	0.573
$\Lambda_8(x) = 0.5x^2 + 0.28x^3 + 0.22x^8$	0.938	0.469	0.59

subsection since P_l is very low. The optimized distributions for different maximum repetition rates $d_{\max}$ are denoted by $\Lambda_{d_{\max}}(x)$ and a regular distribution with repetition rate of 2 along with their corresponding highest asymptotic channel load, G^*, for IRSA, IRA and IRARC are given in Table 3.1. We observe that the ratio of maximum achievable throughput, T^*, between IRSA and IRA is 1/2. We note that this asymptotic relationship is not only particular to irregular repetition rates but also valid for the regular ones as well, and can also be observed through the analysis in Section III. Furthermore, our results show that the optimized distributions of IRSA perform well for both IRA and IRARC [5].

The above behavior for the maximum achievable throughputs between IRSA and IRA deserves more explanation. The failure probabilities at each iteration for IRSA and IRA through the asymptotic analysis can be written as $p_{1,i} = 1-e^{-\mu_{1,i}}$, $p_{2,i} = 1-e^{-2\mu_{2,i}}$ with $\mu_{1,i} = \mu\lambda(p_{1,i-1})$, $\mu_{2,i} = \mu\lambda(p_{2,i-1})$ where $p_{1,i}$ is for IRSA and $p_{2,i}$ are for IRA. Due to the lack of slot synchronization, vulnerable period of a packet in IRA is doubled compared to IRSA. Note that for any given user degree distribution, $\Lambda(x)$ and $\lambda(x)$ functions are the same for the both cases. Thus, for $\mu_{1,i} = 2\mu_{2,i}$, their failure probabilities are equal, and we can write $G_{1,i} = 2G_{2,i}$ by using the load definition $\mu = \Lambda'(1)G$. For the load values smaller than the decoding threshold G^*, the P_l converges to a vanishing value. Then, by using $T^* = (1-P_l)G^*$ and $G^*_{1,i} = 2G^*_{2,i}$, one can obtain $T^*_{IRSA} = 2T^*_{IRA}$. Hence, it is not surprising that the throughput with IRA is half of that of IRSA. We note that

[5]Differential evolution algorithm does not guarantee a globally optimal solution. There exists other distributions perform slightly better for IRARC, however, we did not include them as the improvements were very minor.

while our analysis reveals this simple dependence between the throughputs of IRSA and IRA, this observation is not easy to make without the newly developed machinery.

A similar statement is not straightforward to make for IRARC. Intuitively, we only have a relatively small additional resolution probability because of concatenation that is derived through the same degree distributions, which may be the reason for the optimal distributions for IRA to execute well for IRARC as well.

We now perform finite length simulations for both IRA and IRARC. We evaluate various frame lengths, i.e., 100, 200 and 1000 ms, by assuming that all the replicas have the same length $\tau = 1$ ms. We keep the maximum number of iterations as 20, $i_{\max} = 20$, for all the simulations. We assume ideal SIC throughout our simulations.

We first provide the simulation results of IRA for $\Lambda_8(x)$ and CRA for $\Lambda_2(x)$ by using the above predefined frame lengths in Fig. 3.5 along with the corresponding asymptotic analysis results. The better fit of the finite length simulations and the asymptotic analysis is clearly seen for both throughput and P_l as the frame length increases for $\Lambda_8(x)$. While the analysis is carried out under the asymptotic setting $N, T_f \to \infty$, simulations are performed for finite length scenarios. In the asymptotic setting, each packet replica becomes statistically independent of each other, however this independency does not hold for finite frame lengths. The statistics of replicas become correlated with each other due to the occurrence of loops (stopping sets) which degrade the system performance, and explaining the difference between asymptotic and numerical results.

We observe that the maximum achievable throughput, i.e., the decoding threshold is $G^* = T^* = 0.469$. In addition, the irregular distribution $\Lambda_8(x)$ enhances the throughput by approximately 71% compared to the regular one $\Lambda_2(x)$, asymptotically. For further comparisons, we also examine the asymptotic performance of regular and irregular distributions by keeping the maximum repetition rate fixed as 4 and 5. For the former, $\Lambda(x) = x^4$ and $\Lambda_4(x)$, G^* is increased from 0.386 to 0.434 ($\approx 12\%$). For the latter, $\Lambda(x) = x^5$ and $\Lambda_5(x)$, G^* is increased

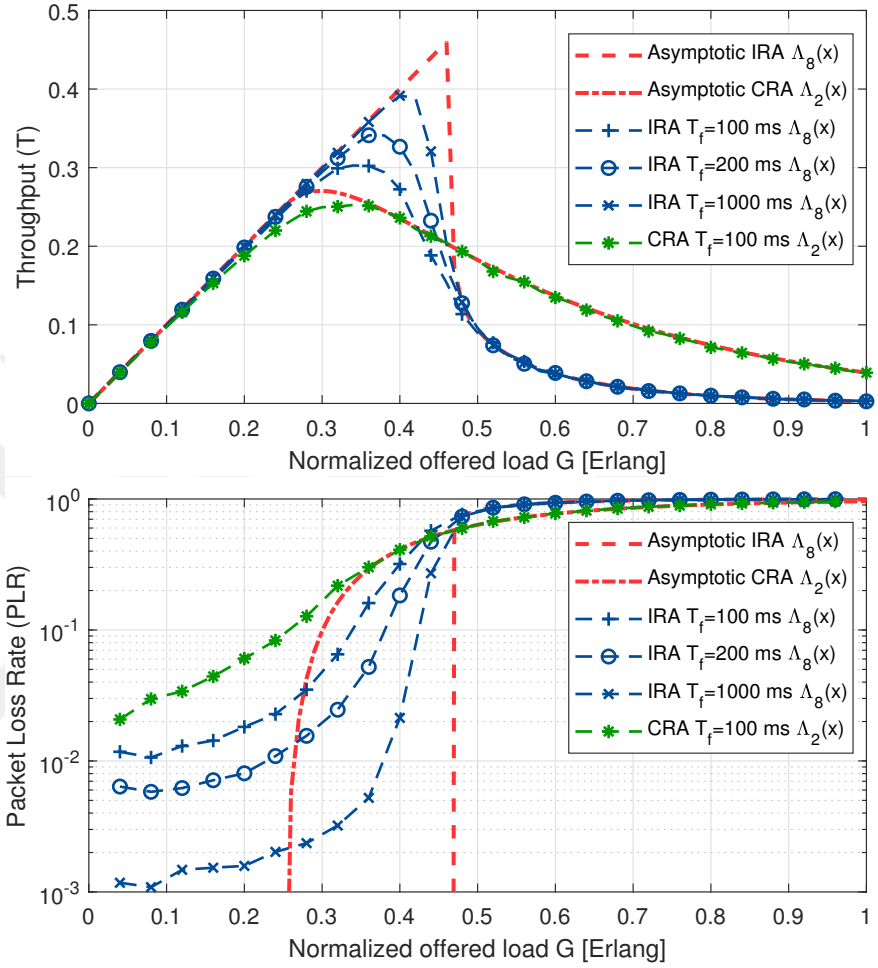

Figure 3.5: Asymptotic analysis of CRA/IRA with $\Lambda_8(x)$ and $\Lambda_2(x)$ for different frame lengths ($T_f = 100, 200, 1000$ ms), $i_{\max} = 20$.

from 0.350 to 0.449 ($\approx 28\%$). Notice that a similar enhancement is also observed for finite length simulations though the percentage improvement is smaller.

We now consider the same set-up with replica concatenation. Fig. 3.6 illustrates the finite length simulation results for $\Lambda_8(x)$ and $\Lambda_2(x)$ along with the asymptotic results of IRA with replica concatenation. We observe that the finite length simulation results comply with the asymptotic analysis, and that the decoding threshold G^* is increased from 0.469 to 0.59. That is, there is a significant improvement (by about 25%) in throughput with replica concatenation. Furthermore, the use of irregular repetition rates offer superior performance as in CRA/IRA.

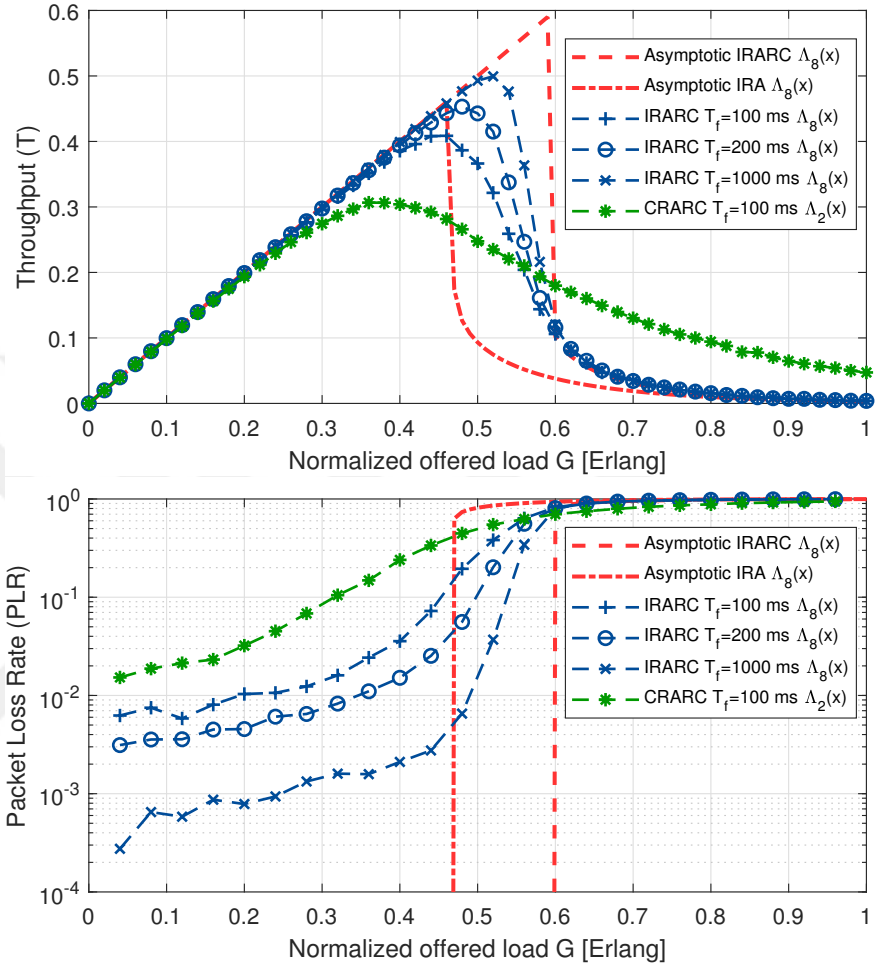

Figure 3.6: Asymptotic analysis of IRARC and IRA with $\Lambda_8(x)$ for different frame lengths ($T_f = 100, 200, 1000$ ms), $i_{\max} = 20$.

Fig. 3.7 depicts the simulation results of CRA and IRA with two replica concatenation, and by employing all possible replicas with $T_f = 200$ ms. As noted earlier, introducing two replica concatenation results in a significant throughput increase compared to CRA/IRA, however, the simulation results show that concatenation of all the replicas performs only slightly better. We explain this as follows: for this specific example, 59% of the packets are resolved with only 1 replica (no concatenation), 30% with 2 replica concatenation, and 9% with 3 replica concatenation (while the remaining percentage is due to concatenation of more replicas) at the specific load value of $G = 0.5$. In other words, it may not be worthwhile to concatenate more than two replicas due to additional complexity,

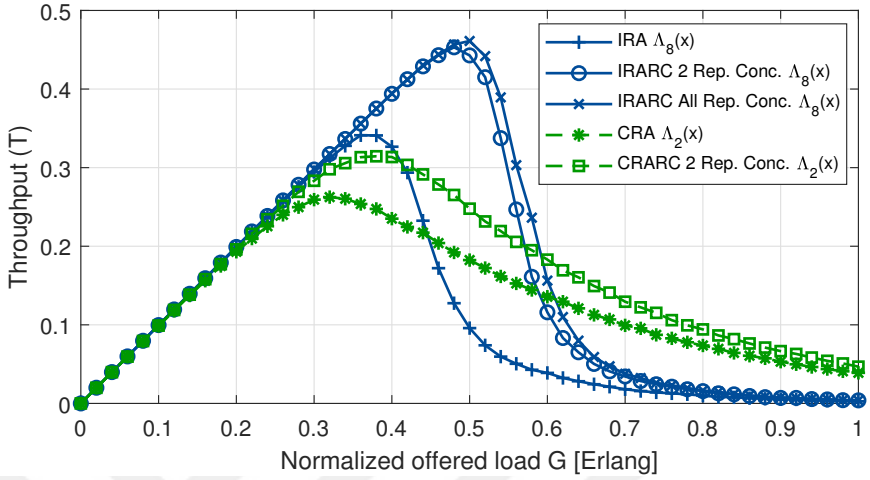

Figure 3.7: Simulation results of CRA/IRA and CRARC/IRARC with 2 and all replica concatenation $\Lambda_8(x)$ and $\Lambda_2(x)$, $T_f = 200$ ms, $i_{\max} = 20$.

as most of the possible gain is already obtained with two. Lastly, in the same plot, we also include supplementary plots for CRA and CRARC with $\Lambda_2(x)$ to depict the additional resolvability, and hence, performance gain introduced by replica concatenation.

We also perform optimization with a constraint on the average repetition rate, $\Lambda'(1)$. In other words, we limit the average transmission power of all active users for different values of $d_{\max}$ and employ differential evolution. The asymptotic performance (G^*) of IRSA, IRA and IRARC for an average repetition rate of at most 3, i.e., $\Lambda'(1) \leq 3$, for different $d_{\max}$ values is given in Table 3.2. We first

Table 3.2: Asymptotic Performance of Distributions for maximum 3 average repetition rate

$d_{\max}$	$\Lambda'(1)$	User Degree Distributions $\Lambda(x)$	IRSA(G^*)	IRA(G^*)	IRARC(G^*)
3	2.81	$\Lambda(x) = 0.1882x^2 + 0.8118x^3$	0.824	0.412	0.513
4	2.98	$\Lambda(x) = 0.5098x^2 + 0.0026x^3 + 0.4876x^4$	0.868	0.434	0.543
5	2.99	$\Lambda(x) = 0.5613x^2 + 0.1619x^3 + 0.2768x^5$	0.887	0.443	0.56
6	2.99	$\Lambda(x) = 0.5613x^2 + 0.1619x^3 + 0.2768x^5$	0.887	0.443	0.56
8	2.99	$\Lambda(x) = 0.5613x^2 + 0.1619x^3 + 0.2768x^5$	0.887	0.443	0.56

note that for $d_{\max}$ values up to 5 the performance is identical to the unconstrained ones. On the other hand, for high values of $d_{\max}$, the performance of the schemes cannot improve any further due to the limit on the average repetition rate.

3.5 Chapter Summary

In this chapter, we propose an asynchronous RA scheme, namely IRA, as an extension to CRA by allowing varying repetition rates, in a similar way to IRSA as a generalization of CRDSA. We present an asymptotic analysis for both CRA and IRA, and show that optimized irregular distributions perform remarkably better than the regular ones. We also propose an enhancement to CRA/IRA by adding replica concatenation capability, which allows merging the clean parts of (two) replicas. We extend the developed analysis of CRA/IRA to the enhanced scheme, and show that replica concatenation provides a significant throughput gain.

Chapter 4

Energy Harvesting IRA and IRARC

In this chapter, we consider a sustainable and practical adaptation of IRA and IRARC for energy harvesting nodes. Different from the previous schemes, energy for the transmissions is provided by the stored energy acquired via EH, therefore, the limitations and stochasticity of energy availability need to be taken into account. In other words, user nodes should satisfy the energy constraint, and the number of replicas should be chosen with respect to the available amount of energy at the beginning of a frame.

We model the available energy by a discrete-time Markov chain and derive optimal transmission policy for given battery state, that will be adopted by all of the active users in order to maximize the overall system throughput through the developed analysis. We also perform simulations to verify the validity of analysis and to show the advantages of optimal policy over other ones.

The chapter is organized as follows. Section 4.1 describes the energy harvesting model employed with IRA and IRARC. In Section 4.2, the design and analysis of IRA and IRARC with energy harvesting are studied. We demonstrate the performance of IRA and IRARC under the energy harvesting constraints in Section

4.3. The summary of chapter is given in Section 4.4.

4.1 Energy Harvesting Model

In the energy harvesting scenario, users are capable of energy harvesting and they are equipped with finite-capacity batteries. We denote the battery capacity by $B_{\max}$. In the proposed system model, we assume that only inactive users can store energy in their batteries during each frame. On the other hand, when users are active, they are not able to harvest energy. This model makes the analysis tractable as the energy arrivals and transmissions occur in different frames and is well-justified for low energy harvesting rates and activity probabilities as the energy arrivals of the active users become very small. For the transmissions, users consume the stored energy (harvested during their inactivity periods).

We assume that each energy arrival brings one unit of energy, and a single replica transmission consumes one unit of energy as well. In general, energy consumption for a replica transmission is relatively high compared to the amount of harvested energy in short time of periods. For example, a sensor node might consume mWs of power for transmission while receiving only uWs from RF harvesting. Our simplified EH model can be generalized to address this imbalance by a proper selection of EH rates as well. The stochastic nature of energy arrivals is governed by a Poisson process with rate α through each frame, where α refers to the expected number of energy arrivals within a frame.

Active users determine their transmission policy according to the battery state at the beginning of each frame in a probabilistic manner. To clarify, users draw the number of replicas to be transmitted within the frame from a certain probability mass function (PMF) determined by the available amount of energy in the battery. For instance, users may prefer to deplete the harvested energy, or alternatively, conserve a certain amount for use in future frames. We emphasize that the repetition rate is not directly drawn from a given PMF as in IRA/IRSA. Instead, it is now determined by the battery state and the transmission policy.

4.2 Asymptotic Analysis

We now present an asymptotic analysis for EH scenario with a finite-sized battery. For the analysis, we first concentrate on determining the amount of energy available in the battery (battery state) for a given user node. We argue that the steady-state distribution of the battery state can easily be computed for a given energy arrival rate α, activation probability π, battery capacity $B_{\max}$ and transmission policy, defined as the transmission probabilities of replica numbers for each battery state. Next, we derive the repetition distribution based on the steady-state distribution of the battery state and the transmission policy.

We consider the battery state only at the beginning of the frames, because the optimal transmission policy can be adopted at that instant. In particular, a user node decides the number of replicas to be sent at the beginning of the frame. Let B_n be the stochastic process that represents the battery state at the beginning of the n-th frame. The battery states at the other time instants are not needed, therefore, we adopt discrete and integer time scale. We assume that the harvested energy arrives stochastically, and follows a Poisson process with rate α. Recall that α refers to the expected number of energy arrivals within a frame. We denote the number of energy arrivals in the n-th frame by E_n, and consequently, its distribution is given by a Poisson PMF. We denote e_k as the probability of k energy arrivals during each frame, i.e.,

$$e_k = \Pr\{E_n = k\} = \frac{e^{-\alpha}\alpha^k}{k!}. \tag{4.1}$$

We now explain the transmission policy that is valid for each active user node. At the beginning of each frame, a user selects the number of replicas to be transmitted probabilistically depending on the state of the battery, B_n. We note that the transmission policy is not specific to a frame, i.e., it is determined in advance and it is known by all the users. We denote the number of replicas that is sent within a frame by a random variable L_k where k units of energy is available in the battery, i.e., $L_k \leq k$ and $B_n = k$. For ease of exposition we define γ_k^l as the

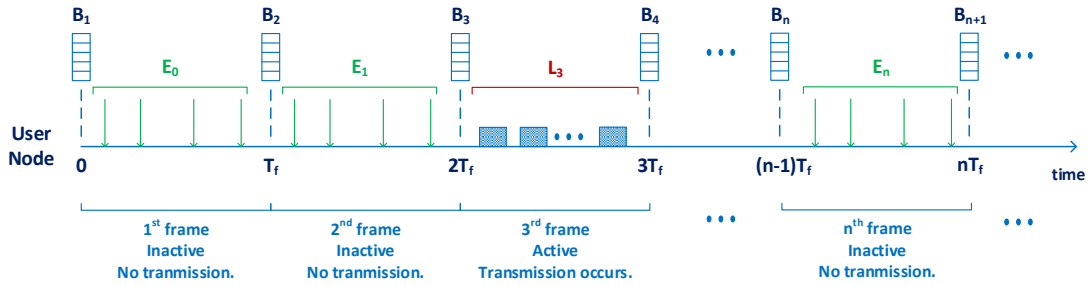

Figure 4.1: A sample from consecutive frames depicting both active and inactive state of a user node.

probability of transmitting l replicas when the battery contains k amounts of unit energy, i.e.,

$$\gamma_k^l = \Pr\{L_k = l \mid B_n = k\}, \text{ s.t. } \sum_{l=0}^{k} \gamma_k^l = 1, \text{ for } k \in \{0, 1, \ldots, B_{\max}\}. \tag{4.2}$$

Up to now, we have described the battery state, the energy arrival process and the transmission policy. The battery state at the next frame can be derived in terms of the current battery state, battery capacity (a constant), the number of unit energy arrivals (if the node is inactive) or the number of unit energy departures due to the transmissions (if the node is active). Hence, the battery state satisfies Markov property, and it is possible to model the stochastic process B_n as a discrete-time Markov chain. However, we have different processes for the active and inactive states of a user as depicted in Fig. 4.1.

During the inactive state of a user node, it only harvests energy, and does not attempt transmission during the frame. On the other hand, in an active state, a user node sends its packet replicas by utilizing the harvested energy in the battery. During the inactive state of a user, we can write B_{n+1} in terms of B_n and E_n as

$$B_{n+1} = \min\{B_n + E_n, B_{\max}\}, \tag{4.3}$$

and the battery state evolves for an active state of a user with k units of energy, $B_n = k$, as follows

$$B_{n+1} = B_n - L_k. \tag{4.4}$$

Next, we define the one-step transition probabilities denoted by δ_{ij} as the probability that the battery is in state j at frame $n+1$ given that the battery was in state i at frame n for $i, j \in \{0, 1, \ldots, B_{\max}\}$. This quantity can be written for the inactive state using (4.3) as

$$\delta_{ij} = \Pr\{B_{n+1} = j \mid B_n = i\} = \begin{cases} \Pr\{E_n = (j-i)\} = e_{(j-i)}, & \text{if } j < B_{\max}, \\ \Pr\{E_n \geq (j-i)\} = \sum\limits_{m=(j-i)}^{\infty} e_m, & \text{if } j = B_{\max}, \end{cases} \tag{4.5}$$

with the condition $j \geq i$ since a user node harvests energy only in the inactive state. Similarly, for the active state we can write transition probabilities using (4.4), i.e.,

$$\delta_{ij} = \Pr\{B_{n+1} = j \mid B_n = i\} = \Pr\{L_i = (i-j)\} = \gamma_i^{(i-j)}, \tag{4.6}$$

with the condition $i \geq j$. Differently from the inactive state, the battery can have at most the same energy with the previous frame since the user node only transmits but does not harvest energy. Then, by utilizing (4.5) and (4.6) with the total probability theorem, we can write the overall one-step transition probabilities in a complete form as follows:

$$\delta_{ij} = \begin{cases} (1-\pi) e_{(j-i)}, & \text{if } j > i \;\&\; j < B_{\max} \\ (1-\pi) \sum\limits_{m=(j-i)}^{\infty} e_m, & \text{if } j > i \;\&\; j = B_{\max} \\ \pi \gamma_i^{(i-j)}, & \text{if } j < i \\ (1-\pi) e_{(j-i)} + \pi \gamma_i^{(i-j)}, & \text{if } j = i \;\&\; j < B_{\max} \\ (1-\pi) \sum\limits_{m=(j-i)}^{\infty} e_m + \pi \gamma_i^{(i-j)} & \text{if } j = i \;\&\; j = B_{\max}. \end{cases} \tag{4.7}$$

Let $\mathbf{P}$ be the one-step transition matrix, where i-th row and j-th column element

being δ_{ij}, given as

$$\mathbf{P} = \begin{bmatrix} (1-\pi)e_0 + \pi\gamma_0^0 & (1-\pi)e_1 & (1-\pi)e_2 & \dots & (1-\pi)\sum_{m=B_{\max}}^{\infty} e_m \\ \pi\gamma_1^1 & (1-\pi)e_0 + \pi\gamma_1^0 & (1-\pi)e_1 & \dots & (1-\pi)\sum_{m=B_{\max}-1}^{\infty} e_m \\ \pi\gamma_2^2 & \pi\gamma_2^1 & (1-\pi)e_0 + \pi\gamma_2^0 & \dots & (1-\pi)\sum_{m=B_{\max}-2}^{\infty} e_m \\ \vdots & \vdots & \vdots & \ddots & \vdots \\ \pi\gamma_{B_{\max}}^{B_{\max}} & \pi\gamma_{B_{\max}}^{B_{\max}-1} & \pi\gamma_{B_{\max}}^{B_{\max}-2} & \dots & (1-\pi)\sum_{m=0}^{\infty} e_m + \pi\gamma_{B_{\max}}^0 \end{bmatrix}$$

where $\mathbf{P} \in \mathbb{R}^{(B_{\max}+1)\times(B_{\max}+1)}$. As a next step, we can derive the steady-state distribution of the battery state denoted by $\boldsymbol{\beta} = [\beta_0,\ \beta_1,\ \dots,\ \beta_{B_{\max}}]$, where

$$\beta_i = \lim_{n\to\infty} \Pr\{B_n = i\}.$$

The steady state distribution can be calculated solving a system of linear equations, i.e., $\boldsymbol{\beta}\mathbf{P} = \boldsymbol{\beta}$ with the following additional conditions, $\sum_{i=0}^{B_{\max}} \beta_i = 1$ and $\beta_i \geq 0$, $\forall i$. We remark that steady state distribution, $\boldsymbol{\beta}$, depends on the energy arrival rate α, the battery capacity $B_{\max}$ and the transmission policy probabilities, γ_k^l. As a last step, we note that we can compute the repetition distribution using the steady state distribution of the battery state and the transmission policy as follows

$$\Lambda_d = \sum_{k=0}^{B_{\max}} \beta_k \gamma_k^d, \text{ for } d \in \{0, 1, \dots, k\}, \tag{4.8}$$

which enables us to perform the asymptotic analysis and evaluate the system performance via the steps already derived for IRA and IRARC in Chapter 3.

We note that asynchronous and coded RA schemes are not satisfactorily energy efficient in terms of the packet transmission attempts compared to synchronous and simple counterparts since redundant transmissions are made to ensure high bandwidth efficiency and lack of synchronization trades the system performance with lower complexity (simple transmitters) and energy requirements for synchronizing massive number of users. Indeed, the main motivation to consider EH with RA is to address the stochasticity of energy arrivals, not to make the schemes more energy efficient.

4.3 Numerical Results

In this section, we study the performance of IRA and IRARC under the energy harvesting constraints with the optimized repetition distributions that take EH into account. We also discuss the effect of parameters $B_{\max}$, α and π on system performance and compare the performance of the optimal policy with the greedy and uniform policies as well.

We now illustrate the asymptotic and numerical results of the aforementioned asynchronous RA schemes by accommodating energy harvesting nodes. For the EH RA schemes, we aim to determine the system parameters in order to maximize the asymptotic throughput, T^*, by employing the developed asymptotic tools in Chapters 3 and 4. Initially, we compute the resulting repetition distribution for given values of $B_{\max}$, α, π and most importantly the transmission probabilities, γ_k^l, by following the steps in Section 4.2. Afterwards, the derived repetition distribution is used to determine asymptotic performance of the system using the developed asymptotic tools of IRA and IRARC in Section III-IV. We note that the repetition distribution optimization is not straightforward as in IRA/IRARC, since the repetition distributions are determined by the steady-state of battery state and the transmission policy. Hence, to maximize the system performance, we optimize the transmission probabilities, γ_k^l, which results in the optimal repetition distributions.

Here, differently from the previous chapter, we perform optimization to maximize the asymptotic throughput, T^*, instead of maximizing G^*, without a constraint on P_l. The reasoning is that, in the case of EH scenario, packet losses are due to not only the collisions, as in IRA and IRARC, but also the packets that are not transmitted (at all) because of energy scarcity. Hence, obtaining vanishing P_l values is not guaranteed for $G \leq G^*$, therefore, T^* is not necessarily equivalent to G^*. For instance, for low values of energy arrival rate, it is not possible to obtain low P_l values since observing energy outages is more likely. In the optimization, we limit the search space with the load values up to the maximum asymptotic load obtained for the non-EH scenario, denoted as $\overline{G}$, and

Table 4.1: Optimized Distributions for given energy arrival rate, $\alpha = 10^{-1}$, and activation probability, $\pi = 10^{-2}$, for different battery capacity values.

$B_{\max}$	User Degree Distributions $\Lambda^b_{B_{\max}}(x)$	EH-IRA (T^*)	EH-IRARC (T^*)
2	$\Lambda^b_2(x) = 0.1x^0 + 0.08x^1 + 0.82x^2$	0.255	0.312
3	$\Lambda^b_3(x) = 0.084x^0 + 0.084x^1 + 0.207x^2 + 0.625x^3$	0.403	0.512
4	$\Lambda^b_4(x) = 0.027x^0 + 0.092x^1 + 0.081x^2 + 0.79x^3 + 0.01x^4$	0.416	0.521
5	$\Lambda^b_5(x) = 0.026x^0 + 0.049x^1 + 0.293x^2 + 0.319x^3 + 0.196x^4 + 0.117x^5$	0.434	0.541
6	$\Lambda^b_6(x) = 0.023x^0 + 0.035x^1 + 0.339x^2 + 0.38x^3 + 0.086x^5 + 0.137x^6$	0.444	0.555
8	$\Lambda^b_8(x) = 0.021x^0 + 0.53x^2 + 0.189x^3 + 0.013x^4 + 0.202x^6 + 0.023x^7 + 0.023x^8$	0.459	0.578

seek for optimal repetition distributions that result in the maximum throughput. Specifically, $\overline{G}$ depends on the battery capacity, $B_{\max}$, and is selected as the maximum G^* value in the corresponding non-EH schemes, provided by $\Lambda_{B_{\max}}$. This approach helps with finding distributions with low P_l values by eliminating the distributions providing similar T^* values with higher channel loads.

Some optimized distributions for different battery capacities, denoted as $\Lambda^b_{B_{\max}}(x)$, and given values of $\alpha = 10^{-1}$ and $\pi = 10^{-2}$ with the corresponding asymptotic throughput values T^* are listed in Table 4.1 [1]. It can be seen that increasing battery capacity enables the user nodes to harvest more energy arrivals into their battery, and hence, allows them to transmit more replicas improving the system performance in a similar way to increasing maximum repetition rate in IRA and IRARC. However, having a higher battery capacity does not necessarily improve the throughput, since for low energy arrival rates, the full capacity may not be even utilized.

Next, we perform finite-length simulations to confirm the validity of the proposed asymptotic analysis. We adopt the same simulation set-up with the previous subsection. As an example, we depict the asymptotic and finite-length performance of the optimized distribution $\Lambda^b_8(x)$ with EH-IRA in Fig. 4.2. As can be observed, the simulation results conform with the asymptotic results obtained through the proposed analysis. It should be noted that for $G \leq G^*$, the P_l

[1] In the optimized distributions, x^0 term stands for active users not transmitting due to energy absence.

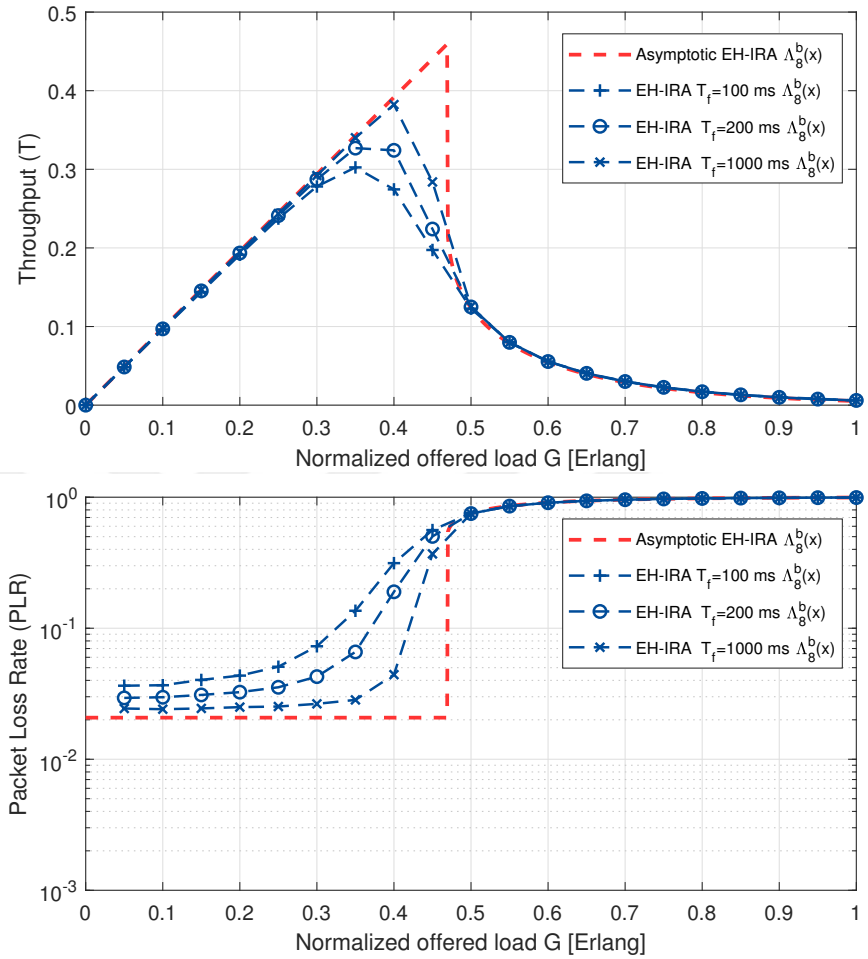

Figure 4.2: Asymptotic analysis of EH-IRA with $B_{\max} = 8$, $\alpha = 10^{-1}$ and $\pi = 10^{-2}$ for different frame lengths ($T_f = 100, 200, 1000$ ms), $i_{\max} = 20$.

is constant and equal to 0.02, which is caused only by the user nodes experiencing energy absence, and in fact, the receiver is able to decode all the transmitted packets through SIC. In addition, the finite-length performance of EH-IRARC also complies with the asymptotic analysis, and the proposed replica concatenation approach increases asymptotic throughput from 0.459 (EH-IRA) to 0.578.

We examine the individual effects of the energy arrival rate α and activation probability π on the system performance for both EH-IRA and EH-IRARC by using the repetition distribution $\Lambda_8^b(x)$. Fig. 4.3a depicts the maximum achievable asymptotic throughput, T^*, and the P_l values for varying energy arrival rates for activity probability $\pi = 10^{-2}$. Similarly, Fig. 4.3b illustrates the asymptotic

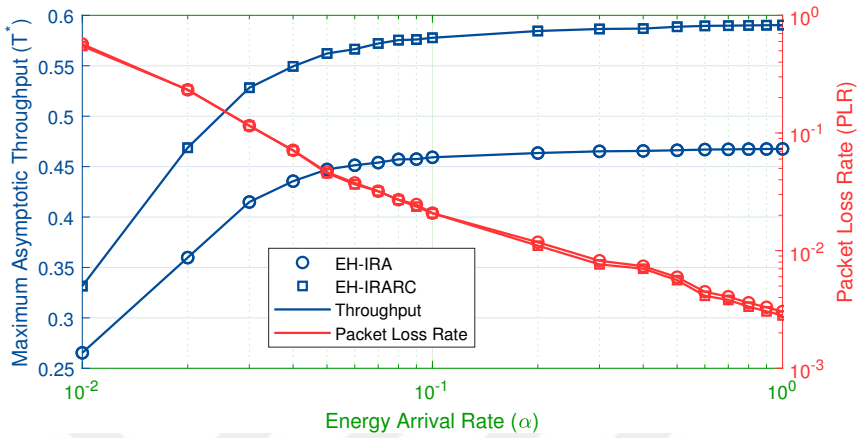

(a)

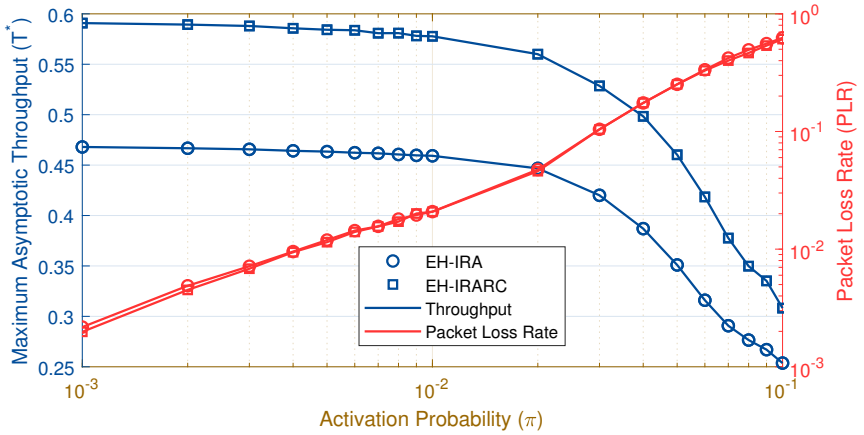

(b)

Figure 4.3: Asymptotic performance of EH-IRA and EH-IRARC with $\Lambda_8^b(x)$ for different energy arrival rates and activation probabilities.

performance for various activation probabilities for a fixed α value, 10^{-1}. It can be seen from Fig. 4.3a that with increasing α values, T^* increases with decreasing P_l, which is due to the fact the more energy harvested from the environment, making energy absence less likely. On the other hand, as shown in Fig. 4.3b, as the activity probability π increases, the system performance deteriorates because the user nodes become active more frequently, which results in shorter inactive periods for energy harvesting. It should also be noted that, the ratio α/π denotes the expected number of energy arrivals during an inactive state. $1/\pi$ denotes the expected number of frames until the user becomes active. Also, α denotes the expected number of energy arrivals for each frame. Hence, α/π represents

total (expected) number of energy arrivals during the inactive state. If this ratio is too low (e.g., $\alpha/\pi < 5$) the system performance deteriorates severely because the user nodes experience more energy shortages, and they can only transmit a limited number of replicas. For larger values of this ratio (e.g., $\alpha/\pi \geq 5$), the improvements are minor due to the limited battery capacity, as most of the energy arrivals are lost. Lastly, EH-IRARC outperforms the EH-IRA in terms of the throughput by allowing higher channel loads, however, the P_l curves are very close to each other since the packet losses are dominated by the user nodes with energy absence which is the same for both schemes.

We also show the advantages of the optimal transmission policy over the other transmission policies. We compare the optimal transmission policy with two naive policies: 1) Greedy transmission policy: User nodes consume all the energy in the battery by transmitting the maximum possible number of replicas, i.e., transmission probabilities for the greedy policy can be written as,

$$\gamma_k^l = \begin{cases} 1, & \text{if } l = k, \\ 0, & \text{otherwise,} \end{cases}$$

for $k \in \{0, 1, \ldots, B_{\max}\}$. 2) Uniform transmission policy: User nodes choose a number for the replicas, which is allowed by the available energy, uniformly, i.e.,

$$\gamma_k^l = \frac{1}{(k+1)},$$

for $k \in \{0, 1, \ldots, B_{\max}\}$. For example, if a battery contains 3 units of energy, in the greedy policy, a node transmits 3 replicas; whereas in the uniform policy, a node can send 0, 1, 2 or 3 replicas with probability, 1/4 each. We provide the optimal transmission probabilities for $B_{\max} = 8$, $\alpha = 10^{-1}$ and $\pi = 10^{-2}$ as, $\gamma_0^0 = 1$, $\gamma_1^0 = 1$, $\gamma_2^2 = 1$, $\gamma_3^2 = 0.992$, $\gamma_3^3 = 0.008$, $\gamma_4^2 = 1$, $\gamma_5^2 = 0.982$, $\gamma_5^3 = 0.018$, $\gamma_6^2 = 0.565$, $\gamma_6^3 = 0.435$, $\gamma_7^2 = 0.443$, $\gamma_7^3 = 0.026$, $\gamma_7^4 = 0.188$, $\gamma_7^6 = 0.343$, $\gamma_8^2 = 0.436$, $\gamma_8^3 = 0.229$, $\gamma_8^6 = 0.302$, $\gamma_8^8 = 0.033$ and zero otherwise.

Table 4.2: Optimized Distributions of different transmission policies given $B_{\max} = 8$, $\alpha = 10^{-1}$ and $\pi = 10^{-2}$.

Transmission Policy	User Degree Distributions $\Lambda(x)$	EH-IRA (T^*)
Greedy	$\Lambda_g(x) = 0.1x^0 + 0.08x^1 + 0.07x^2 + 0.07x^3 + 0.06x^4 + 0.06x^5 + 0.05x^6 + 0.05x^7 + 0.46x^8$	0.343
Uniform	$\Lambda_u(x) = 0.16x^0 + 0.14x^1 + 0.13x^2 + 0.12x^3 + 0.11x^4 + 0.1x^5 + 0.09x^6 + 0.08x^7 + 0.07x^8$	0.422
Optimal	$\Lambda_o(x) = 0.02x^0 + 0.53x^2 + 0.19x^3 + 0.01x^4 + 0.2x^6 + 0.03x^7 + 0.02x^8$	0.459

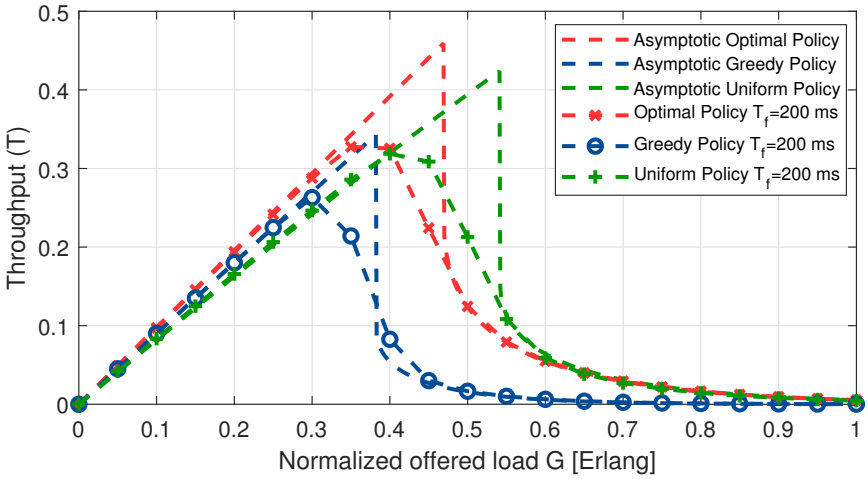

Figure 4.4: Asymptotic throughput performance of greedy, uniform and optimal policies for EH-IRA with $B_{\max} = 8$, $\alpha = 10^{-1}$ and $\pi = 10^{-2}$ with frame length 200 ms and $i_{\max} = 20$.

We present the resulting repetition distributions corresponding to the respective transmission policies in Table 4.2. The asymptotic performance of the transmission policies along with the finite length simulation results for EH-IRA is illustrated in Fig. 4.4. In the greedy policy, users consume all the energy in the battery which results in the distributions with higher probabilities in more replicas. This approach is not favorable for the system performance since collisions are more likely with more replicas. We should note that greedy policy suffers from transmitting maximum number of replicas (8) for modest and high load values. However, for lower load values, transmitting replicas with higher repetitions is beneficial by decreasing PLR. In the uniform policy, the corresponding repetition distribution provides better throughput than the greedy policy as it saves energy for the following rounds and less collisions occur thanks to the uniform selection. On the other hand, it leads to higher P_l due to the users selecting

to transmit no replicas. Furthermore, we note that the uniform policy can offer better throughput values for higher loads, since no replica transmission is more probable compared to the optimal policy. However, this is not a desired behavior, since it is always possible to increase maximum load values G^* with more packet loss keeping the throughput the same. The optimal policy minimizes the percentage of users suffering from the energy absence, which in fact results in a smaller P_l, and provides a better throughput performance compared to the other policies.

4.4 Chapter Summary

In this chapter, we consider an energy limited scenario for users, and propose a practical energy harvesting model for IRA and IRARC. We analyze the proposed energy harvesting RA scheme considering stochasticity of the available energy, and derive an optimal transmission policy through the developed model aiming at improving the system performance. We also consider different transmission policies, greedy and uniform, to demonstrate the excellence of the optimal one. Finally, the asymptotic analysis results are corroborated with extensive finite length simulations.

Chapter 5

IRA with Packet Length Diversity

In this chapter, we propose a generalized version of the asynchronous random access scheme IRA. In the proposed scheme, users are allowed to transmit their packets with varying durations independently from each other in such a way that the overall system throughput is increased. We present an asymptotic throughput analysis of the newly proposed scheme when it is used together with time diversity, i.e., by repetition of the users' packets. We also optimize the probability distributions governing the repetition rates and packet durations with the aid of the developed analysis. We demonstrate that the optimized distributions achieve considerably higher throughputs than those achievable by IRA only, and we verify the asymptotic results via finite length simulations.

The chapter is organized as follows. In Section 5.1, we specify the system model. Section 5.2 develops the analysis for IRA with packet length diversity. In Section 5.3, we optimize the probability distributions for packet lengths and repetition rates, and provide the corresponding asymptotic system performance in comparison with that of IRA. We also present finite frame length simulation results in the same section. Finally, Section 5.4 concludes the chapter.

5.1 System Model

IRA-PLD is a generalization of IRA, hence it adopts the system model in Chapter 3 with the exception that we now consider packet length diversity as well. In this section, we briefly mention the main features of the scheme to make the chapter self-contained.

We consider an asynchronous random access protocol where users transmit multiple copies of their packets to a single receiver over a common MAC frame. We assume that packets of different users can be of different lengths, and that the users are not synchronized at a slot-level, however, we still assume that transmissions are frame synchronous. The total number of users is N_t and each user is activated with probability π independently from each other per each frame. The expected number of active users is denoted by N, i.e., $N = \pi N_t$ and the length of the MAC frame is T_f. Each active user sends multiple copies of its packet at different time instants selected uniformly at random over the frame, and the number of replicas for each user is drawn in a probabilistic manner independently of each other. We also assume that each active user randomly chooses its own packet length (hence the length of its replicas) from a set of available levels independently of the other users in the system [1]. The channel occupancy generated by all the users, normalized load G, is defined as the expected duration of the total packet transmissions divided by the frame length, i.e.,

$$G = \frac{N \cdot \bar{\tau}}{T_f},$$

where $\bar{\tau}$ denotes the average packet length over all users.

We consider a collision channel model that is commonly employed in RA schemes. In this setup, a packet can be in two states: interfered or interference-free, which can be detected by the receiver. Due to the asynchronism, the collisions are mostly partial unlike the slotted schemes, however, we still assume that even when a small portion of a packet interferes it is not resolvable at the receiver.

[1] We note that the packet length determines the amount of information that can be transmitted inside of a packet, and hence, users with higher packet duration transmit more information.

When a packet is interference-free, it is always successfully decoded. Whenever a packet is decoded, its copies are eliminated through SIC, hence the interference caused by it is completely removed from the frame[2]. The receiver proceeds with the decoding process iteratively until there is no interference-free packet in the frame or a maximum number of iterations is reached.

5.2 Asymptotic Analysis

We present an asymptotic convergence analysis of the system under consideration. We conduct the analysis by letting the frame length and the number of active users go to infinity ($N, T_f \rightarrow \infty$) while keeping the channel traffic, $G = \frac{N \cdot \bar{\tau}}{T_f}$, constant. This asymptotic setting allows for two simplifications that make the problem tractable: 1) the packet arrivals follow as a Poisson process with density G; 2) the positions of packet replicas become statistically independent of each other. The statistics of packet replicas, namely, their resolvability/non-resolvability probabilities, are only identified by the packet lengths due to their specific vulnerable periods as will be discussed explicitly. Using the developed analysis which enables us to assess the asymptotic system performance for a given packet length/repetition distribution, we also search for optimal distributions that maximize the throughput for a given channel load.

We now develop an asymptotic convergence analysis for IRA with packet length diversity. Specifically, we are interested in studying the overall system performance for a given packet length/repetition distribution utilizing an approach similar to the one employed in the equal packet length case. As a first step, we define $\Phi_{d,m}$ as the probability that a user transmits d replicas each with length τ_m. As in IRA, let Λ_d denote the probability of a user sending d replicas where $d = 1, 2, \ldots, D$. We also define Γ_m as the probability that a user selects a packet of length τ_m chosen from a set $\mathcal{T}$ of M available lengths, i.e., $\mathcal{T} = \{\tau_1, \tau_2, \ldots, \tau_M\}$,

[2]Note that to adopt SIC, we assume that each packet has position information of its replicas and this information is accurate enough to locate the transmission times of the replicas. The packet length information is also needed to remove the interference of replicas.

$m = 1, 2, \ldots, M$. Clearly, we can obtain Λ_d and Γ_m by using $\Phi_{d,m}$ as

$$\Lambda_d = \sum_{m=1}^{M} \Phi_{d,m}, \qquad \Gamma_m = \sum_{d=1}^{D} \Phi_{d,m}.$$

The average packet repetition rate, $\bar{d}$, and average packet length, $\bar{\tau}$, can be found as

$$\bar{d} = \sum_{d=1}^{D} \sum_{m=1}^{M} d\Phi_{d,m} = \sum_{d=1}^{D} d\Lambda_d,$$
$$\bar{\tau} = \sum_{d=1}^{D} \sum_{m=1}^{M} \tau_m \Phi_{d,m} = \sum_{m=1}^{M} \tau_m \Gamma_m.$$

Next, we compute the probability that a randomly selected replica belongs to a user sending its packets with d replicas and its packet length is τ_m, denoted by $\phi_{d,m}$, as

$$\phi_{d,m} = \frac{d\Phi_{d,m}}{\bar{d}}.$$

In addition, we also define γ_m as the probability that a randomly selected replica has a packet length τ_m in terms of $\phi_{d,m}$, i.e.,

$$\gamma_m = \sum_{d=1}^{D} \phi_{d,m} = \frac{\sum_{d=1}^{D} d\Phi_{d,m}}{\bar{d}}.$$

We define the user and replica degree distributions using the packet and replica probabilities $\Phi_{d,m}$ and $\phi_{d,m}$ in a polynomial form for each packet length by normalizing with Γ_m and γ_m as

$$\Phi_m(x) \triangleq \frac{1}{\Gamma_m} \sum_{d=1}^{D} \Phi_{d,m} x^d, \qquad \phi_m(x) \triangleq \frac{1}{\gamma_m} \sum_{d=1}^{D} \phi_{d,m} x^{d-1},$$

for $m = 1, 2, \ldots, M$. Clearly, we can write the user and replica degree distributions in a more compact form as

$$\Phi(\mathbf{x}) \triangleq \sum_{d=1}^{D} \sum_{m=1}^{M} \Phi_{d,m} {x_m}^d, \qquad \phi(\mathbf{x}) \triangleq \sum_{d=1}^{D} \sum_{m=1}^{M} \phi_{d,m} {x_m}^{d-1},$$

where $\mathbf{x} = [x_1, x_2, \ldots, x_M]^T$ is an $M \times 1$ vector of indeterminate variables.

We focus on an arbitrary replica with length τ_s, and denote the probability that this replica is not resolved at iteration i by $p_{s,i}$, $s = 1, 2, \ldots, M$. Condition on the event that there are l_m packet replica arrivals with length τ_m inside the vulnerable period of the chosen replica, $m = 1, 2, \ldots, M$, and define $q_{m,i}$ as the average non-resolvability probability of replica arrivals with length τ_m at the previous iteration $(i-1)$. This probability can be calculated by considering different users that utilize length τ_m packets with different repetition rates, i.e., by averaging over $\phi_{d,m}$ as

$$q_{m,i} = \frac{1}{\gamma_m} \sum_{d=1}^{D} \phi_{d,m} p_{m,i-1}^{d-1} = \phi_m(p_{m,i-1}).$$

In order to resolve the chosen replica, all the replica arrivals with different packet lengths that collide with it must be resolved. That is, the probability that the replica under consideration will be not resolved is given by

$$p_{s,i} = 1 - \prod_{m=1}^{M} (1 - q_{m,i})^{l_m} = 1 - \prod_{m=1}^{M} (1 - \phi_m(p_{m,i-1}))^{l_m}. \tag{5.1}$$

Next, we specify the vulnerable period of the replica with length τ_s as depicted in Fig. 5.1 in comparison with the standard IRA. We emphasize that the vulnerable period of the chosen packet is particular for each packet length. In other words, we cannot identify the vulnerable period in a general form that is valid for all cases. Hence, we denote the vulnerable period of the replica with length τ_s by $(\tau_s + \tau_m)$ for a replica of length τ_m interfering with the one under consideration.

The packet replica arrivals of length τ_m follow a Poisson process with density

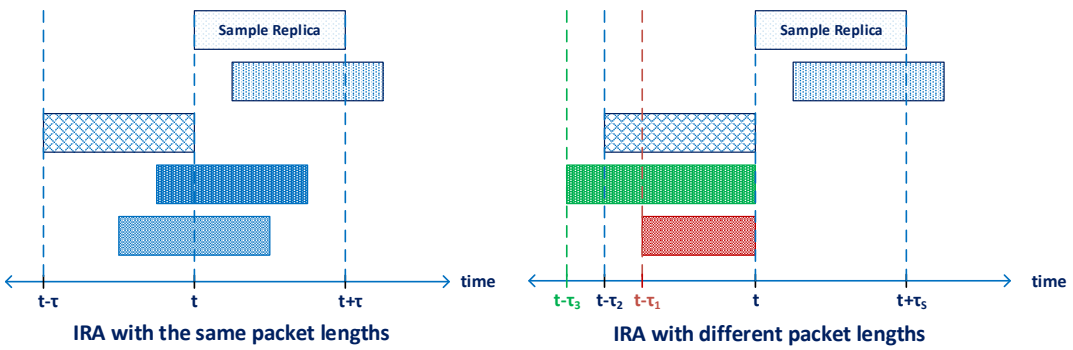

Figure 5.1: Vulnerable period comparison of standard IRA and IRA with different packet lengths.

$\bar{d}\gamma_m G$ under the asymptotic setting $(N, T_f \to \infty)$. Thus, the distribution of the number of replica arrivals, l_m, is given by a Poisson random variable. For simplicity of notation, we define G' as the number of packet replica arrivals per unit length, i.e., $G' = \frac{G}{\bar{\tau}}$. We then denote the probability of l_m replica arrivals within their respective vulnerable period $(\tau_s + \tau_m)$ by ρ_{l_m}, i.e.,

$$\rho_{l_m} = e^{-\bar{d}\gamma_m G'(\tau_s+\tau_m)} \frac{(\bar{d}\gamma_m G'(\tau_s+\tau_m))^{l_m}}{l_m!}. \tag{5.2}$$

Next, we compute $p_{s,i}$ by averaging (5.1) over the statistics of the packet replica arrivals ρ_{l_m}, and obtain

$$\begin{aligned}
p_{s,i} &= \prod_{m=1}^{M} \sum_{l_m=0}^{\infty} \rho_{l_m} \left(1 - \prod_{m=1}^{M} (1 - \phi_m(p_{m,i-1}))^{l_m}\right) \\
&= \prod_{m=1}^{M} \sum_{l_m=0}^{\infty} \left(e^{-\bar{d}\gamma_m G'(\tau_s+\tau_m)} \frac{(\bar{d}\gamma_m G'(\tau_s+\tau_m))^{l_m}}{l_m!}\right) \left(1 - \prod_{m=1}^{M} (1 - \phi_m(p_{m,i-1}))^{l_m}\right) \\
&= 1 - \prod_{m=1}^{M} e^{-\bar{d}\gamma_m G'(\tau_s+\tau_m)\phi_m(p_{m,i-1})} \\
&= 1 - e^{-\sum_{m=1}^{M} \bar{d}\gamma_m G'(\tau_s+\tau_m)\phi_m(p_{m,i-1})}.
\end{aligned}$$

To describe $p_{s,i}$ in a more explicit manner, let $\mu_{m,i}$ denote the unresolved load at iteration i formed by the replicas with length τ_m. We can write $\mu_{m,i} =$

$\bar{d}\gamma_m G'\phi_m(p_{m,i-1})$, and obtain

$$\begin{aligned} p_{s,i} &= 1 - e^{-\sum_{m=1}^{M} \mu_{m,i}(\tau_s+\tau_m)} \\ &= 1 - e^{-\tau_s \sum_{m=1}^{M} \mu_{m,i}} e^{-\sum_{m=1}^{M} \tau_m \mu_{m,i}}. \end{aligned} \tag{5.3}$$

In this expression, the term $\tau_s \sum_{m=1}^{M} \mu_{m,i}$ corresponds to the total unresolved load (with all possible packet lengths) within the duration of the chosen packet length τ_s, which is independent of the length of the interfering packets. On the other hand, the term $\sum_{m=1}^{M} \tau_m \mu_{m,i}$ accounts for the unresolved load within the respective durations τ_m of the interfering packets, and hence it is computed for each packet length separately. To conclude, the exponential terms in (5.3) denote the probability of no arrivals from the unresolved load for their corresponding intervals.

Another observation is that as the packet length increases, it is more likely that the replica will collide with the other users' packets (due to its wider vulnerable period), hence its non-resolvability probability, $p_{s,i}$, is increased compared to those with lower durations. Hence, we can state that $q_{k,i} \geq q_{l,i}$ for any $\tau_k \geq \tau_l$ at an arbitrary iteration i.

Finally, we evaluate the system performance using two metrics, packet loss rate (PLR) and normalized throughput T. We define the PLR for each specific packet length, denoted by P_l^m, as the ratio of the number of users utilizing a packet length τ_m being not successfully resolved to the number of all users with the same packet length. That is,

$$P_l^m = \frac{1}{\Gamma_m} \sum_{d=1}^{D} \Phi_{d,m}(p_{m,i_{\max}})^d = \Phi_m(p_{m,i_{\max}}).$$

We define the normalized throughput T by considering the total lengths of the packets (total number of channel symbols) received correctly over the entire frame

normalized by the frame length T_f. That is,

$$T = \frac{N}{T_f}\sum_{m=1}^{M}\Gamma_m\tau_m(1-P_l^m)$$
$$= G\left(1-\sum_{d=1}^{D}\sum_{m=1}^{M}\Phi_{d,m}\frac{\tau_m}{\bar{\tau}}(p_{m,i_{\max}})^d\right).$$

The metrics PLR and T for the standard IRA are simplified versions of the above general definitions since the packets are of equal length. Namely, in this case, $\Lambda_d = \Phi_{d,m}$, $\Gamma_m = 1$ and $\tau = \bar{\tau}$. Hence, PLR and throughput are simply given by $P_l = \Lambda(p_{i_{max}})$ and $T = (1-P_l)G$, respectively.

We have developed a tool to determine the asymptotic PLR and normalized throughput of IRA with packet length diversity for a given repetition and packet length distribution. We can utilize the developed analysis to optimize the distributions that should be used as well. To do this, for a given maximum repetition rate D and available packet length set $\mathcal{T}$, we search for the optimal probability distributions, $\Phi(\mathbf{x})$, that maximize the asymptotic throughput over possible load values by using a differential evolution algorithm [13]. This is similar to what is done in the optimization process of IRSA [12] and IRA [5].

5.3 Numerical Results

We now study the proposed scheme of IRA with different packet lengths through the developed asymptotic performance analysis and finite frame length simulations. The optimal distributions are obtained for different maximum repetition rates $D = 4, 5, 6, 8$, and packet durations are chosen from $\mathcal{T} = \{\tau', 2\tau', 3\tau', 4\tau', 5\tau'\}$. The optimized distributions with different maximum repetition rates along with their maximum channel loads G^* are presented in Table 5.1. We also provide the optimized distributions of IRA which do not take packet length diversity into account (i.e., when all the packets have equal length τ), as a benchmark. The results show that the proposed scheme offers a superior

Table 5.1: Optimized repetition and packet length distributions.

Length/Repetition Distributions $\Phi(\mathbf{x})$	IRA-PLD (G^*)	Repetition Distributions $\Lambda(x)$	IRA (G^*)
$\Phi_4(\mathbf{x}) = 0.189x_4^2 + 0.811x_1^4$	0.475	$\Lambda_4(x) = 0.5102x^2 + 0.4898x^4$	0.434
$\Phi_5(\mathbf{x}) = 0.1809x_5^2 + 0.1012x_2^3 + 0.7179x_1^5$	0.505	$\Lambda_5(x) = 0.5631x^2 + 0.0436x^3 + 0.3933x^5$	0.449
$\Phi_6(\mathbf{x}) = 0.1973x_5^2 + 0.1494x_3^3 + 0.6533x_1^6$	0.522	$\Lambda_6(x) = 0.5465x^2 + 0.1623x^3 + 0.2912x^6$	0.457
$\Phi_8(\mathbf{x}) = 0.1821x_5^2 + 0.1975x_4^3 + 0.6204x_1^8$	0.540	$\Lambda_8(x) = 0.5x^2 + 0.28x^3 + 0.22x^8$	0.469

performance, and the use of different packet lengths enhances the asymptotic performance allowing for higher achievable asymptotic channel loads.

We perform finite frame length simulations for different channel loads and compute the normalized throughput and packet loss rate to evaluate the system performance as well. We set the maximum number of iterations, $i_{\max}$, to 20. We normalize the packet lengths for given repetition and packet length distributions, to keep the load definition consistent with that used in IRA and the slotted random access schemes, $\bar{\tau} = \sum_{m=1}^{M} \Gamma_m \tau_m = \tau$. We calculate the number of users attempting transmission for given frame length and load value as $N = \frac{G \cdot T_f}{\bar{\tau}}$, and take $\bar{\tau} = 1$ ms. We assume an ideal SIC throughout our simulations.

As a first set of simulations, we consider different frame lengths, 100 ms, 200 ms and 1000 ms, and assume that the distribution $\Phi_8(\mathbf{x})$ is employed. The optimized distribution, $\Phi_8(\mathbf{x})$, adopts packets lengths of $\tau_1 = 0.4309$ ms, $\tau_4 = 1.7235$ ms and $\tau_5 = 2.1543$ ms to satisfy the constraint $\sum_{m=1}^{M} \Gamma_m \tau_m = 1$ ms. Note that $\Phi_8(\mathbf{x})$ utilizes only these lengths. The results are depicted in Fig. 5.2 along with the expected asymptotic performance. It is clear that the finite length simulation results approach the asymptotic performance as the frame length increases, and hence, they confirm the validity proposed analysis in a non-asymptotic (practical) setting. We note that the asymptotic throughput T^* is almost equal to the channel load up to G^*, and then it decays swiftly where we observe a rapid increase in the PLR.

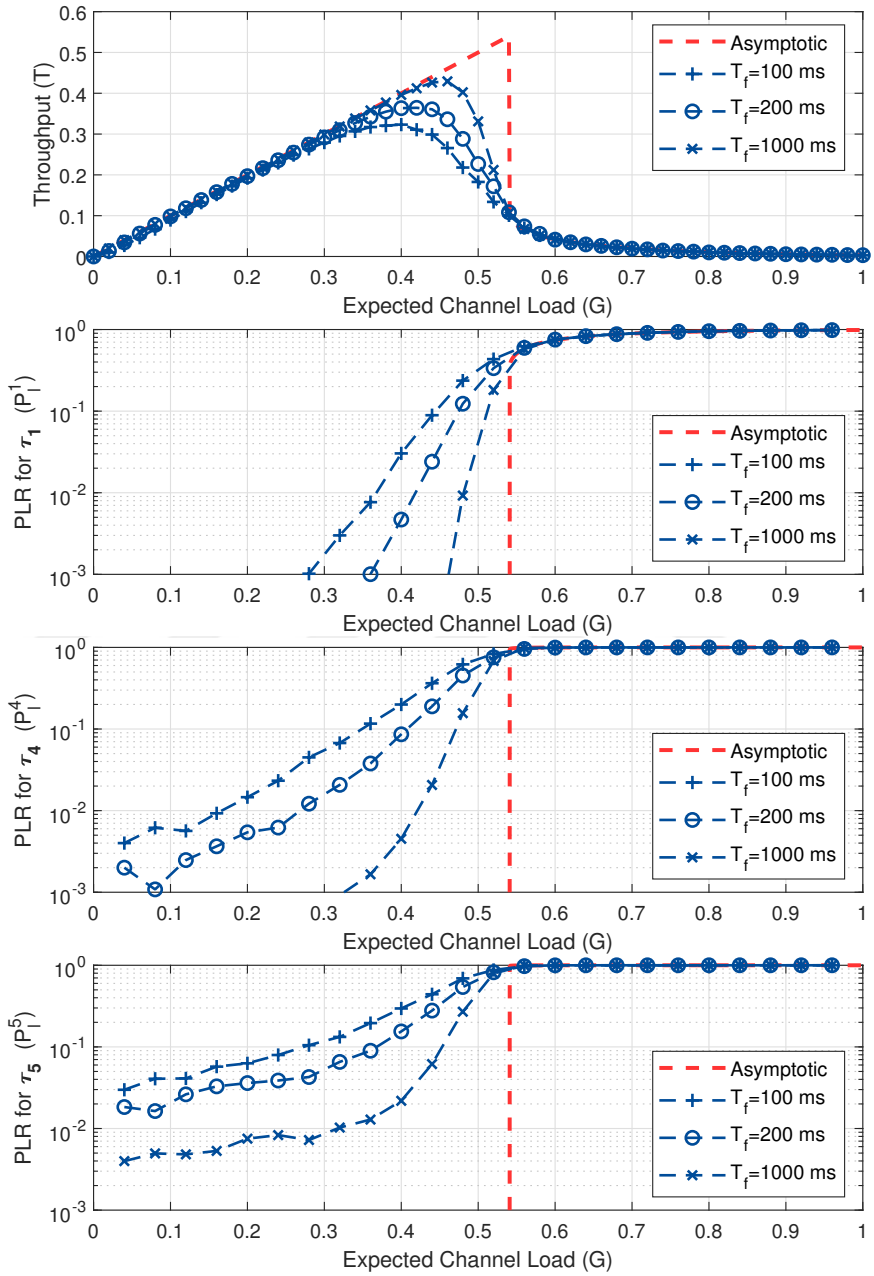

Figure 5.2: Asymptotic analysis of IRA with packet length diversity for $\Phi_8(\mathbf{x})$ with different frame lengths ($T_f = 100, 200, 1000$ ms), $i_{max} = 20$.

We also compare the PLRs corresponding to different packet lengths and observe that the PLR performance degrades as the packet length increases because a packet with a longer duration is more likely to collide due to its broader vulnerable period (resulting in a higher non-resolvability probability, and hence a larger

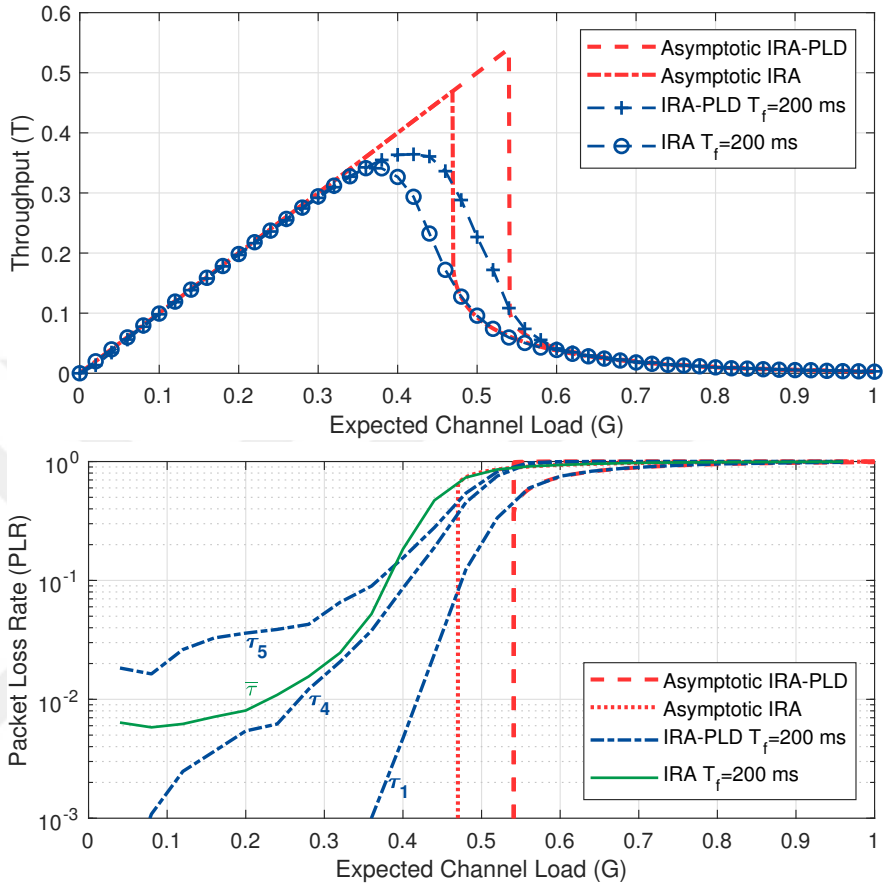

Figure 5.3: Performance Comparison of IRA with packet length diversity for $\Phi_8(\mathbf{x})$ and IRA for $\Lambda_8(x)$ with $T_f = 200$ ms, $i_{max} = 20$.

PLR). Consequently, sending a packet with a lower duration is advantageous in terms of the PLR, however, as a trade-off, such a selection limits the amount of information that can be transmitted. We also observe that the asymptotic PLR performances are almost identical up to G^*, however, after this point they differ from each other (which is not clearly observable in the figure). As a specific example, for a load of $G = 0.6$, the PLR values are 0.7412, 0.9973 and 0.9995 for the three different length packets, respectively.

Finally, we compare the asymptotic performance of IRA with packet length diversity with $\Phi_8(\mathbf{x})$ and that of standard IRA with $\Lambda_8(x)$ in Fig. 5.3. The figure also depicts the finite length simulation results for a frame length of 200 ms. Clearly, the proposed scheme outperforms the standard IRA as it is able

to exploit the packet length diversity and offers a higher achievable asymptotic channel load G^*, increasing the normalized throughput from 0.469 to 0.54 (a gain of nearly 15%). We note that the gains observed in finite length simulations are smaller compared to the asymptotic settings. We also note that the PLR values corresponding to τ_1 and τ_4 remain lower than that of IRA with packet length $\bar{\tau}$ for the chosen frame length. The same observation holds for packets of length τ_5 for the load values larger than 0.4. Clearly, for moderate channel loads, the proposed scheme allows for all the packets of different lengths to be received successfully with higher probabilities compared to the standard IRA.

5.4 Chapter Summary

In this chapter, we have introduced an enhancement of the asynchronous irregular random access scheme by utilizing different packet lengths providing additional diversity. We develop an asymptotic convergence analysis of the enhanced scheme accommodating different packet lengths for a given packet length/repetition distribution. With the help of the developed approach and a suitable differential evolution algorithm, we also obtain optimized distributions for packet durations and repetition rates leading to higher throughputs compared to those offered by standard IRA. The results demonstrate that the system performance is significantly improved compared to that of IRA due to the additional diversity offered by the use of different packet lengths.

Chapter 6

Conclusions and Future Directions

In this thesis, we have studied asynchronous RA protocols with different configurations.

In Chapter 3, we study an asynchronous RA scheme (namely, IRA) with the motivation that such schemes can allow users to transmit their packets at arbitrary time instants within a frame, and hence, they remove the stringent slot synchronization requirements among users. We also propose an enhancement to IRA to benefit from the partial interferences caused by slot asynchronism. We show that it is possible to obtain an interference free packet by concatenating the free parts of the replicas which allows receiver to continue the SIC process even none of the replicas are fully interference free. We present an asymptotic analysis of both IRA and IRARC, and show that the optimized solutions obtained with the aid of asymptotic tools and differential evolution perform well in both schemes.

In Chapter 4, we study IRA and IRARC with energy harvesting nodes where each node is capable of harvesting energy from the environment and store it in its finite-capacity battery. In this scenario, the design and analysis of these schemes

is conducted under the setting of stochastic availability of energy. We derive an optimal transmission policy for different values of system parameters, i.e., battery capacity, energy arrival rate and activation probability, and show the excellence of the optimal policy in comparison with other approaches. We also perform simulations to corroborate the validity of the developed analysis, and assess the system performance for the practical scenarios through finite length simulations.

In Chapter 5, we consider IRA by allowing users to transmit their packets with varying durations independently from each other, i.e., packet lengths are not restricted to be equal. We present an asymptotic analysis of the newly proposed scheme by generalizing the developed analysis for IRA to the case allowing for different packet lengths. With the help of the analysis, we find the optimal packet length and repetition distributions which improve the throughput of IRA. We demonstrate that the additional diversity offered by the use of different packet lengths to the repetition of packets contributes highly to the overall system performance.

We now describe several possible research directions on the general topic of asynchronous RA protocols studied in this thesis.

One possible future research direction is to evaluate the system performance with different metrics, e.g., delay and spectral efficiency, instead of throughput. Different from mMTC, delay is very critical for ultra-reliable low-latency communications (URLLC) in 5G communication systems. Hence for such applications, when the number of active users is low, using longer frame lengths might be unnecessary, and hence, adopting varying frame lengths might be a solution to decrease the overall system delay.

Another line of work can be to study the performance of asynchronous RA protocols for different channel models. In this thesis, we have adopted the destructive collision channel model where a collision is not resolvable. In asynchronous protocols, this model is highly pessimistic because the collisions are mostly partial and with the application of FEC codes, a certain amount of interference can be tolerated. Hence, more optimistic channels models for asynchronous RA protocols

may be preferred [34]. Moreover, different channel models, e.g., fading channel and erasure channel, can be used in the analysis of asynchronous RA protocols as a future research direction as well.

One can also study other coded asynchronous RA protocols. In our study, we have only considered the repetition of packets, however, different coding schemes can also be applied. For example, in CSA [14], linear block codes are utilized instead of repetition codes and it is shown that it is more energy efficient than IRSA and it performs better in terms of throughput for a certain regime of interest. Hence, one may find it appealing to study the design and analysis of different coding schemes for the unslotted counterpart of CSA. Another direction might be to work on new coding schemes for a practical implementation of the set-up in [28] as it is shown that there is still a large gap to the capacity limit with the present approaches. While approaches with superior coding algorithms and slotted ALOHA schemes can be studied, it is also interesting to consider unslotted schemes as well as energy harvesting scenarios in this framework.

In addition, one may also find interesting to study unslotted RA protocols with different packet power levels with a suitable channel model. In [19], it is demonstrated that the use of additional power diversity with optimization yields a better performance for the slotted scenario; we expect that there would be some improvement for the unslotted case as well.

Finally, in our study, we have used a relatively simple EH model to keep the analysis of the problem tractable. It may be interesting to consider other EH models as well, however, the design and analysis of more complicated EH models might be challenging. Moreover, EH integrated coded RA protocols might be appealing as well. One can study the performance of RA protocols with a proper design of a coding scheme with EH. For example, taking the energy availability into account, users may prefer to select lower code rates since some of the coded segments might not be transmitted due to the energy limitations.

Bibliography

[1] F. Boccardi, R. W. Heath Jr, A. Lozano, T. L. Marzetta, and P. Popovski, "Five disruptive technology directions for 5G," *IEEE Commun. Mag.*, vol. 52, no. 2, pp. 74–80, Feb. 2014.

[2] M. Agiwal, A. Roy, and N. Saxena, "Next generation 5G wireless networks: A comprehensive survey," *IEEE Commun. Surveys Tuts.*, vol. 18, no. 3, pp. 1617–1655, 3rd Quart., 2016.

[3] E. Casini, R. De Gaudenzi, and O. Del Rio Herrero, "Contention resolution diversity slotted ALOHA (CRDSA): An enhanced random access scheme for satellite access packet networks," *IEEE Trans. Wirel. Commun.*, vol. 6, no. 4, pp. 1408–1419, Apr. 2007.

[4] S. Sudevalayam and P. Kulkarni, "Energy harvesting sensor nodes: Survey and implications," *IEEE Commun. Surveys Tuts.*, vol. 13, no. 3, pp. 443–461, 3rd Quart. 2011.

[5] T. Akyıldız, U. Demirhan, and T. M. Duman, "Asymptotic analysis of contention resolution ALOHA with replica concatenation," in *Proc. IEEE Int. Conf. Commun. (ICC)*, Shanghai, China, May 2019.

[6] T. Akyıldız and T. M. Duman, "Irregular repetition ALOHA with packet length diversity," in *Proc. IEEE Glob. Telecommun. Conf. (GLOBECOM)*, Waikoloa, HI, USA, Dec. 2019.

[7] N. Abramson, "The ALOHA system: Another alternative for computer communications," in *Proc. Fall Joint Comput. Conf.*, 1970, pp. 281–285.

[8] D. Bertsekas and R. Gallager, *Data Networks*. Englewood Cliffs, NJ, USA: Prentice-Hall, 1992.

[9] L. G. Roberts, "ALOHA packet system with and without slots and capture," *ACM SIGCOMM Comput. Commun. Rev.*, vol. 5, no. 2, pp. 28–42, Apr. 1975.

[10] G. L. Choudhury and S. S. Rappaport, "Diversity ALOHA – a random access scheme for satellite communications," *IEEE Trans. Commun.*, vol. 31, no. 3, pp. 450–457, Mar. 1983.

[11] O. del Rio Herrero and R. De Gaudenzi, "A high-performance MAC protocol for consumer broadband satellite systems," in *Proc. 27th AIAA Int. Commun. Satellite Syst. Conf. (ICSSC)*, Edinburgh, UK, Jun. 2009.

[12] G. Liva, "Graph-based analysis and optimization of contention resolution diversity slotted ALOHA," *IEEE Trans. Commun.*, vol. 59, no. 2, pp. 477–487, Feb. 2011.

[13] R. Storn and K. Price, "Differential evolution - a simple and efficient heuristic for global optimization over continuous spaces," *J. Glob. Optim.*, vol. 11, no. 4, pp. 341–359, Dec. 1997.

[14] E. Paolini, G. Liva, and M. Chiani, "Coded slotted ALOHA: A graph-based method for uncoordinated multiple access," *IEEE Trans. Inf. Theory*, vol. 61, no. 12, pp. 6815–6832, Dec. 2015.

[15] C. Stefanovic and P. Popovski, "ALOHA random access that operates as a rateless code," *IEEE Trans. Commun.*, vol. 61, no. 11, pp. 4653–4662, Nov. 2013.

[16] K. R. Narayanan and H. D. Pfister, "Iterative collision resolution for slotted ALOHA: An optimal uncoordinated transmission policy," in *Proc. 7th Int. Symp. Turbo Codes Iterative Inf. Process. (ISTC)*, Gothenburg, Sweden, Aug. 2012.

[17] F. Clazzer, E. Paolini, I. Mambelli, and C. Stefanovic, "Irregular repetition slotted ALOHA over the Rayleigh block fading channel with capture," in *Proc. IEEE Int. Conf. Commun. (ICC)*, Paris, France, May 2017.

[18] A. Mengali, R. De Gaudenzi, and P.-D. Arapoglou, "Enhancing the physical layer of contention resolution diversity slotted ALOHA," *IEEE Trans. Commun.*, vol. 65, no. 10, pp. 4295–4308, Oct. 2017.

[19] S. Alvi, S. Durrani, and X. Zhou, "Enhancing CRDSA with transmit power diversity for machine-type communication," *IEEE Trans. on Veh. Technol.*, vol. 67, no. 8, pp. 7790–7794, 2018.

[20] M. Ivanov, F. Brännström, A. Graell i Amat, and P. Popovski, "Error floor analysis of coded slotted ALOHA over packet erasure channels," *IEEE Commun. Lett.*, vol. 19, no. 3, pp. 419–422, March 2015.

[21] Z. Sun, Y. Xie, J. Yuan, and T. Yang, "Coded slotted ALOHA for erasure channels: Design and throughput analysis," *IEEE Trans. on Commun.*, vol. 65, no. 11, pp. 4817–4830, Nov. 2017.

[22] S. Gollakota and D. Katabi, "ZigZag decoding: Combating hidden terminals in wireless networks," in *Proc. ACM SIGCOMM Conf. Data Commun.*, Seattle, WA, USA, 2008.

[23] J. Paek and M. J. Neely, "Mathematical analysis of throughput bounds in random access with ZigZag decoding," in *Proc. 7th Int. Symp. on Modeling and Opt. in Mobile, Ad Hoc, and Wirel. Netw. (WiOpt)*, Seoul, Korea, Jun. 2009.

[24] S. Ogata and K. Ishibashi, "Application of ZigZag decoding in frameless ALOHA," *IEEE Access*, vol. 7, pp. 39 528–39 538, 2019.

[25] M. Oinaga, S. Ogata, and K. Ishibashi, "Design of coded ALOHA with ZigZag decoder," *IEEE Access*, vol. 7, pp. 168 527–168 535, 2019.

[26] E. Sandgren, A. Graell i Amat, and F. Brännström, "On frame asynchronous coded slotted ALOHA: Asymptotic, finite length, and delay analysis," *IEEE Trans. on Commun.*, vol. 65, no. 2, pp. 691–704, 2017.

[27] A. Graell i Amat and G. Liva, "Finite-length analysis of irregular repetition slotted ALOHA in the waterfall region," *IEEE Commun. Lett.*, vol. 22, no. 5, pp. 886–889, May 2018.

[28] Y. Polyanskiy, "A perspective on massive random-access," in *Proc. IEEE Int. Symp. Inf. Theory (ISIT)*, Jun. 2017.

[29] O. Ordentlich and Y. Polyanskiy, "Low complexity schemes for the random access Gaussian channel," in *Proc. IEEE Int. Symp. Inf. Theory (ISIT)*, Jun. 2017.

[30] A. Vem, K. R. Narayanan, J. Cheng, and J. Chamberland, "A user-independent serial interference cancellation based coding scheme for the unsourced random access Gaussian channel," in *Proc. IEEE Inf. Theory Workshop (ITW)*, Nov. 2017.

[31] M. Kazemi, T. M. Duman, and M. Médard, "Double-zipper: Multiple access with ZigZag decoding," in *Proc. IEEE Int. Conf. Commun. (ICC)*, Jun. 2020.

[32] C. Kissling, "Performance enhancements for asynchronous random access protocols over satellite," in *Proc. IEEE Int. Conf. Commun. (ICC)*, Kyoto, Japan, Jun. 2011.

[33] F. Clazzer and C. Kissling, "Enhanced contention resolution ALOHA - ECRA," in *Proc. 9th Int. ITG Conf. Syst. Commun. Coding (SCC)*, vol. 9, Munich, Germany, Nov. 2013.

[34] F. Clazzer, C. Kissling, and M. Marchese, "Enhancing contention resolution ALOHA using combining techniques," *IEEE Trans. Commun.*, vol. 66, no. 6, pp. 2576–2587, Jun. 2018.

[35] R. McEliece and W. Stark, "Channels with block interference," *IEEE Trans. on Inform. Theory*, vol. 30, no. 1, pp. 44–53, Jan. 1984.

[36] M. Moradian and F. Ashtiani, "Throughput analysis of a slotted ALOHA-based network with energy harvesting nodes," in *Proc. IEEE 23rd Int. Symp.*

on Pers. Indoor and Mobile Radio Commun. (PIMRC), Sydney, NSW, Australia, Sep. 2012, pp. 351–356.

[37] M. Moradian and F. Ashtiani, "Sum throughput maximization in a slotted ALOHA network with energy harvesting nodes," in *Proc. IEEE Wirel. Commun. and Netw. Conf. (WCNC)*, Istanbul, Turkey, April 2014, pp. 1585–1590.

[38] J. Jeon and A. Ephremides, "On the stability of random multiple access with stochastic energy harvesting," *IEEE J. Sel. Areas Commun.*, vol. 33, no. 3, pp. 571–584, Mar. 2015.

[39] F. Iannello, O. Simeone, and U. Spagnolini, "Medium access control protocols for wireless sensor networks with energy harvesting," *IEEE Trans. Commun.*, vol. 60, no. 5, pp. 1381–1389, May 2012.

[40] D. Shaviv, P. Nguyen, and A. Özgür, "Capacity of the energy-harvesting channel with a finite battery," *IEEE Trans. on Inf. Theory*, vol. 62, no. 11, pp. 6436–6458, Nov. 2016.

[41] F. Vázquez-Gallego, J. Alonso-Zarate, and L. Alonso, "Reservation dynamic frame slotted-ALOHA for wireless M2M networks with energy harvesting," in *Proc. IEEE Int. Conf. Commun. (ICC)*, London, UK, Jun. 2015.

[42] F. Iannello, O. Simeone, P. Popovski, and U. Spagnolini, "Energy group-based dynamic framed ALOHA for wireless networks with energy harvesting," in *Proc. 46th Annu. Conf. Inf. Sci. Syst. (CISS)*, Princeton, NJ, USA, March 2012.

[43] F. Iannello, O. Simeone, and U. Spagnolini, "Dynamic framed-ALOHA for energy-constrained wireless sensor networks with energy harvesting," in *Proc. IEEE Glob. Telecommun. Conf. (GLOBECOM)*, Miami, Florida, USA, Dec. 2010.

[44] S. Ulukus, A. Yener, E. Erkip, O. Simeone, M. Zorzi, P. Grover, and K. Huang, "Energy harvesting wireless communications: A review of recent advances," *IEEE J. Sel. Areas in Commun.*, vol. 33, no. 3, pp. 360–381, Mar. 2015.

[45] U. Demirhan and T. M. Duman, "Energy-harvesting irregular repetition slotted ALOHA with unit-sized battery," in *Proc. IEEE Int. Conf. Commun. (ICC)*, Kansas City, USA, May 2018.

[46] U. Demirhan and T. M. Duman, "Irregular repetition slotted ALOHA with energy harvesting nodes," *IEEE Trans. Wirel. Commun.*, vol. 18, no. 9, pp. 4505–4517, Sep. 2019.

[47] R. De Gaudenzi, O. del Rio Herrero, G. Acar, and E. Garrido Barrabes, "Asynchronous contention resolution diversity ALOHA: Making CRDSA truly asynchronous," *IEEE Trans. Wirel. Commun.*, vol. 13, no. 11, pp. 6193–6206, Nov. 2014.

[48] M. Abramowitz and I. A. Stegun, *Handbook of Mathematical Functions with Formulas, Graphs, and Mathematical Tables*. New York: Dover, 1964.